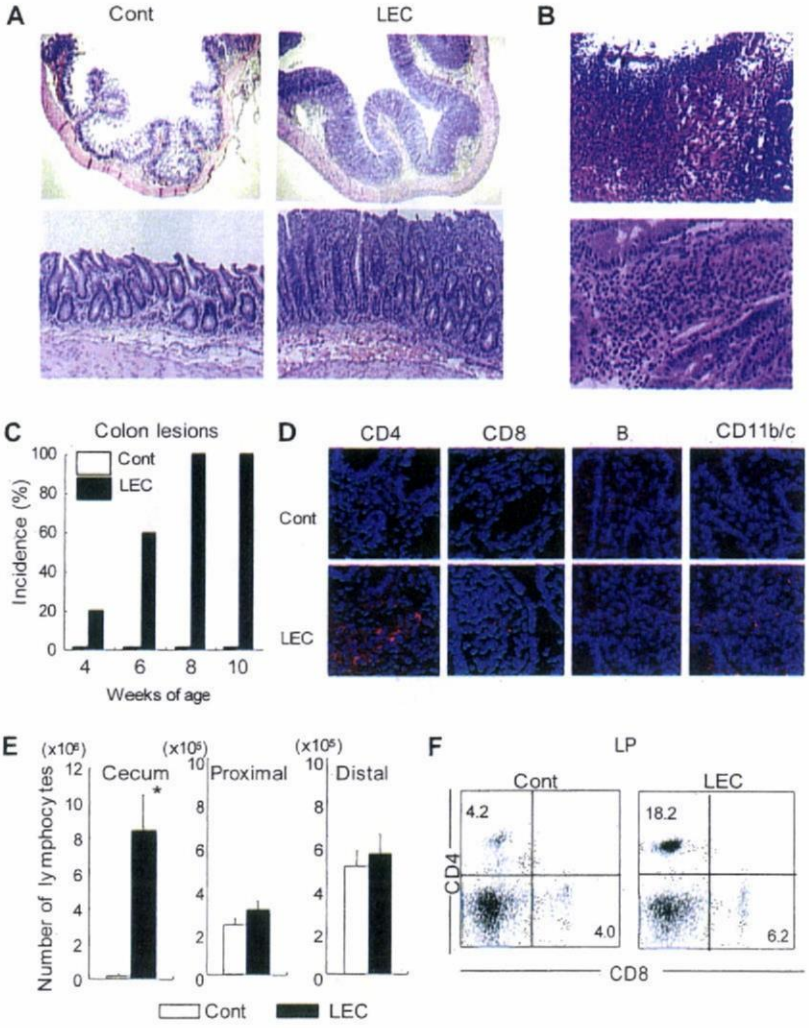

FIGURE 1. IBD-like lesion of LEC rats. *A*, Pathology of colon lesions from LEC and control rats. The thickened wall of colon was found in LEC rats. Inflammatory findings with lymphocyte infiltration were observed in cecum sections from LEC, not control rats, at 8 wk of age. Representative photomicrographs (original magnification, ×20 and 100) of H&E-stained paraffin section from LEC and control rats are shown. *B*, Development of IBD-like lesions of LEC rats. Ulceration and mononuclear cell infiltration was found in the colon lesions of LEC rats. Representative photomicrographs (original magnification, ×100 and 200) of H&E-stained paraffin section of colon from LEC rats are shown. *C*, Incidence of IBD-like lesions in LEC rats. The incidence of IBD-like lesions of LEC and control rats at 4–10 wk of age was evaluated by histological analysis. Complete absence of colon lesions in control rats was found. Approximately four to nine rats were analyzed for each age. *D*, Immunohistochemical analysis of infiltrating cells into colon lesions of LEC rats. Staining with anti-CD4, -CD8, -CD45R, and -CD11b/c was performed using the sections from LEC and control rats at 8 wk of age. Alexa 568 (red) as the second Ab and DAPI (blue) for nuclear staining was used. Photos are representative of three to five samples (original magnification, ×630). *E*, The number of LP lymphocytes in cecum, proximal, and distal colon tissues from LEC and control rats was evaluated. The number of cells was shown as mean (percent) ± SD from five to eight rats in each group. *, $p < 0.0005$ LEC vs control rats. *F*, T cell subsets of LP lymphocytes in the lesions of LEC rats. Flow cytometric analysis was performed with LP lymphocytes of cecum from LEC and control rats of 8 wk of age. A representative result of five samples is shown.

GCCAGACTTTGT-3′ and reverse, 5′-TCCACTTTCGCTGATGAC ACA-3′. Results were calculated by a software of DNA Engine Opicon System (Roche Molecular System).

Statistics

The Student *t* test was used for statistical analysis. Values of $p > 0.05$ were considered significant.

Results

Pathology of colon lesion of LEC rats

Histopathological analysis of all organs of LEC rats from 4 to 12 wk of age was performed. Thickened LP of the colon from LEC rats was observed relative to that from control LEA rats (Fig. 1*A*). Ulcer formation with fibrin exudates, mononuclear cell, and neutrophil infiltration was observed in the surface of the lesion (Fig. 1*B*, *upper*). In the thickened LP of LEC rats, mononuclear cell infiltration was prominent (Fig. 1*B*, *lower*). Most severe inflammatory lesions were seen in the tissue around the cecum in LEC rats. Although the precise mechanisms as to why the most severe lesion developed in the tissue around the cecum of LEC rats is unclear, it is possible that the differential bacterial distribution from the other segments of colon or unique mucosal immunity of cecum may influence the cecum lesion of LEC rats. No inflammatory lesions in LEC rats were observed in the other organs in general. The colon lesions developed spontaneously in almost 100% of LEC rats at 8 wk of age or more, and the incidence of lesions was consistently increased with aging (Fig. 1*C*). There was no sex difference in the colon lesions of LEC rats. LEC rats have also been reported as an animal model for Wilson's disease because of the genetic copper metabolism disorder (36). It is known that the body weight of LEC rats is significantly reduced compared with that of control rats because of the disease (37). Therefore, it is unclear whether the IBD-like lesions of the LEC rat may influence the loss of body weight.

To clarify the population of the immune cells infiltrated in the LP of IBD-like lesions from LEC rats, immunohistochemical analysis was performed using the cecum sections from LEC rats. We found that $CD4^+$ T cells and $CD11b/c^+$ macrophages or dendritic cells were mainly infiltrated, and a small number of $CD45R^+$ B and $CD8^+$ T cells were also found in the lesions of LEC rats (Fig. 1*D*). The total cell number of lymphocytes in the LP of cecum among colon from LEC rats was significantly higher than that from control rats (Fig. 1*E*). However, there was no difference in number of LP mononuclear cells (LPMCs) in proximal and distal colon between control and LEC rats (Fig. 1*E*). Moreover, flow cytometric analysis with T lymphocytes in the LP of the lesions revealed that the prominent population was $CD4^+$ T cells compared with those of control rats (Fig. 1*F*).

Characteristics of T cells from LEC rats

To examine the immunological characteristics in LEC rats, the thymocytes and peripheral T cells were analyzed. We found that

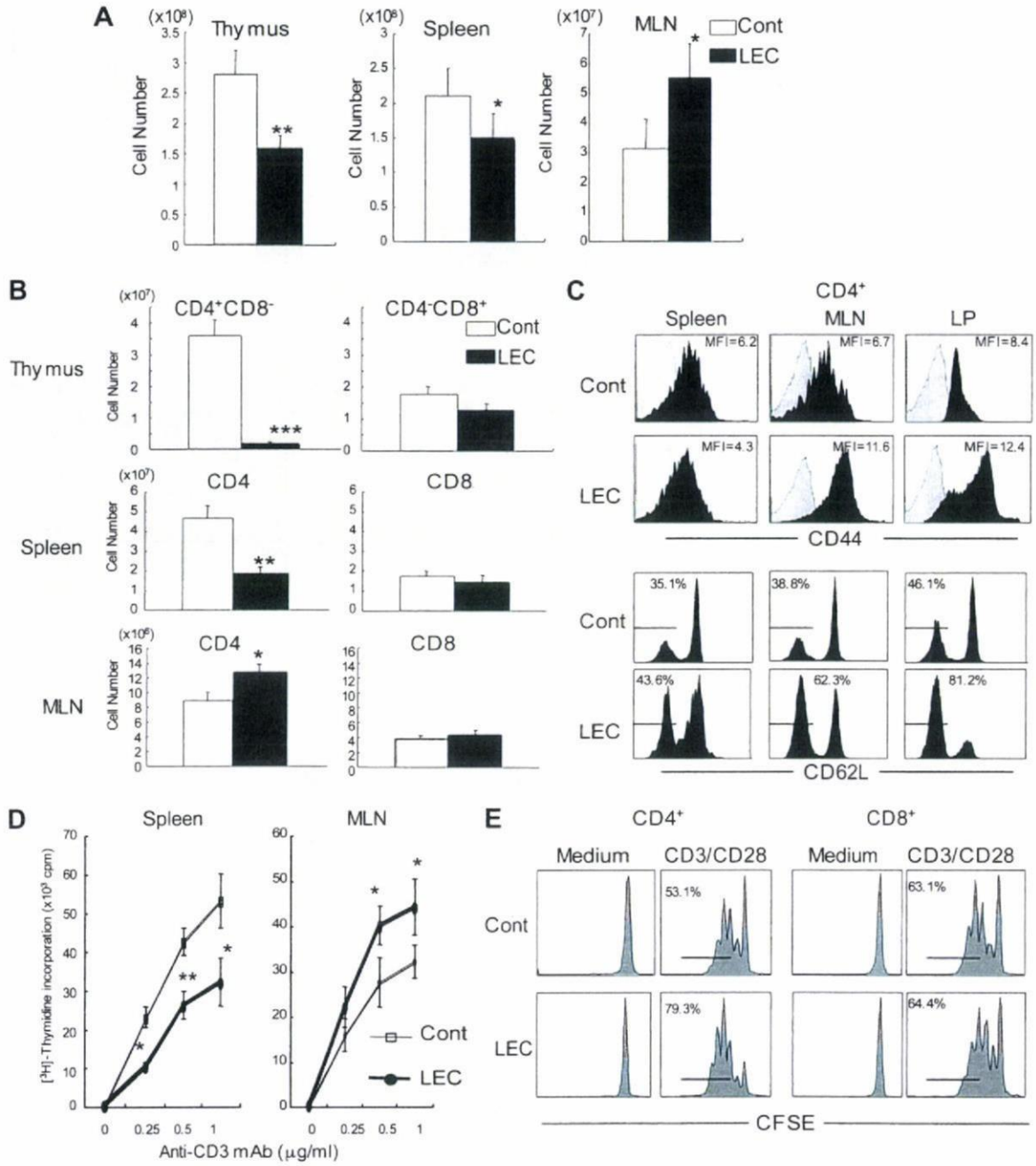

FIGURE 2. Characteristics of T cells from LEC rats. *A*, The cell number of the thymus, spleen, and MLNs are shown as mean ± SD from five to seven LEC and control rats of at 2 mo of age. *, $p < 0.05$; **, $p < 0.0005$ LEC vs control rats. *B*, T cell subsets of the thymus, spleen, and MLNs from LEC rats. Flow cytometric analysis was performed using thymocytes, spleen cells, and MLN cells. The number of $CD4^+$ or $CD8^+$ T cells was shown as mean (percent) ± SD from five to eight rats in each group. *, $p < 0.0005$; **, $p < 0.00005$; ***, $p < 0.0000005$ LEC vs control rats. *C*, Activation of $CD4^+$ T cells from LEC rats. CD44 and CD62L expressions on $CD4^+$ T cells of spleen and MLNs from control and LEC rats were analyzed by flow cytometric analysis. Mean fluorescence intensity (MFI) of CD44 expression is shown. $CD62L^-$ cells (percent) are indicated in the panels. Results are representative of three samples. *D*, Proliferative responses were analyzed by [^{3}H]thymidine incorporation using spleen and MLN T cells stimulated with plate-coated CD3 mAb (0~1 μg/ml) and CD28 mAb (5 μg/ml) for 72 h. The data are shown as the mean ± SD of three triplicate samples. Graphs are representative of three independent experiments. *, $p < 0.05$; **, $p < 0.005$ LEC vs control rats. *E*, Purified T cells from MLNs of control and LEC rats were labeled with CFSE (0.5 μM), and stimulated with CD3 mAb (1 μg/ml) and CD28 mAb (5 μg/ml) for 72 h. CFSE dilution of $CD4^+$ and $CD8^+$ T cells was estimated by flow cytometry. Graphs are representative of three independent experiments.

the cell number of thymus and spleen from LEC rats was significantly lower than that from control rats, while the cell number of MLNs was significantly higher compared with that from control rats (Fig. 2*A*). Significant reduction of $CD4^+CD8^-$ cells of the thymus and $CD4^+$ T cells of the spleen from LEC rats was observed in contrast to the populations from control rats as described in the previous report (Fig. 2*B*) (32). In contrast, there was a greater increase of $CD4^+$ T cell number of MLNs found in LEC rats compared with that from control rats (Fig. 2*B*). No significant change for $CD8^+$ T cells was observed in the thymus, spleen, and MLNs (Fig. 2*B*). In addition, CD44 expression, one of the activation markers for T cells, on $CD4^+$ T cells of MLNs and LP from LEC rats was significantly higher than that from control rats (Fig. 2*C*). Also, $CD62L^-CD4^+$ T cells, which are memory phenotype,

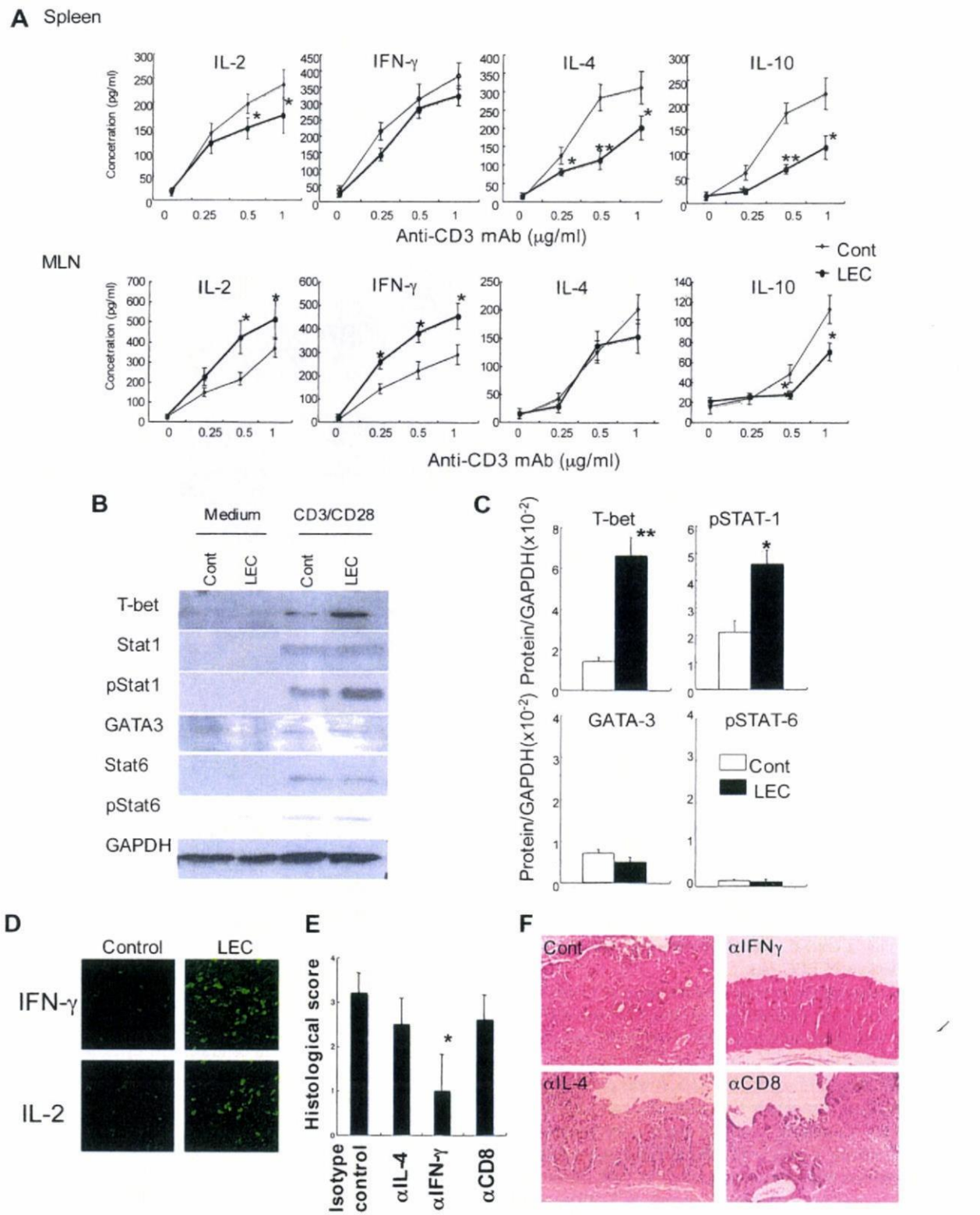

FIGURE 3. Cytokine switching of LEC rats. *A*, Purified T cells of the spleen and MLNs from LEC and control rats were stimulated with CD3 mAb (0~1 μg/ml) and CD28 mAb (5 μg/ml) for 24 h. The culture supernatants were analyzed for cytokine productions including IL-2, IFN-γ, IL-4, and IL-10 by ELISA. The concentration was shown as the mean ± SD of three triplicate samples. Graphs are representative of two independent experiments. *, $p < 0.05$; **, $p < 0.005$ LEC vs control rats. *B*, Purified T cells of MLNs from control and LEC rats were stimulated with CD3-CD28 ligation for 24 h. The cell lysates were used for the expression of T-bet and GATA-3, and the expression and phosphorylation of STAT-1 and STAT-6. GAPDH was used as a housekeeping protein. The photos are shown as representative results from three samples. *C*, Protein quantification of cytokine-switching molecules was performed using chemiluminescence images. Relative expressions to GAPDH were calculated. Results are mean ± SD of three samples. *, $p < 0.05$; **, $p < 0.005$ LEC vs control rats. *D*, IFN-γ and IL-2 expressions of colon were detected by immunofluorescence staining with the first mAbs and Alexa 488-conjugated anti-mouse IgG as the second Ab. The photos are shown as representative results from three samples. *E*, The neutralizing mAbs (50 μg/rat) and isotype control Ab (50 μg/rat) were i.v. injected twice a week into LEC rats from 8 to 10 wk of age. Colonic histology scores of experimental rats are shown. Data are mean ± SD of four to six rats per group. *, $p < 0.05$ treated vs control Ab treated. *F*, Sections of colons from neutralizing Ab-treated LEC rats were stained with PAS. Photos are representative of each group.

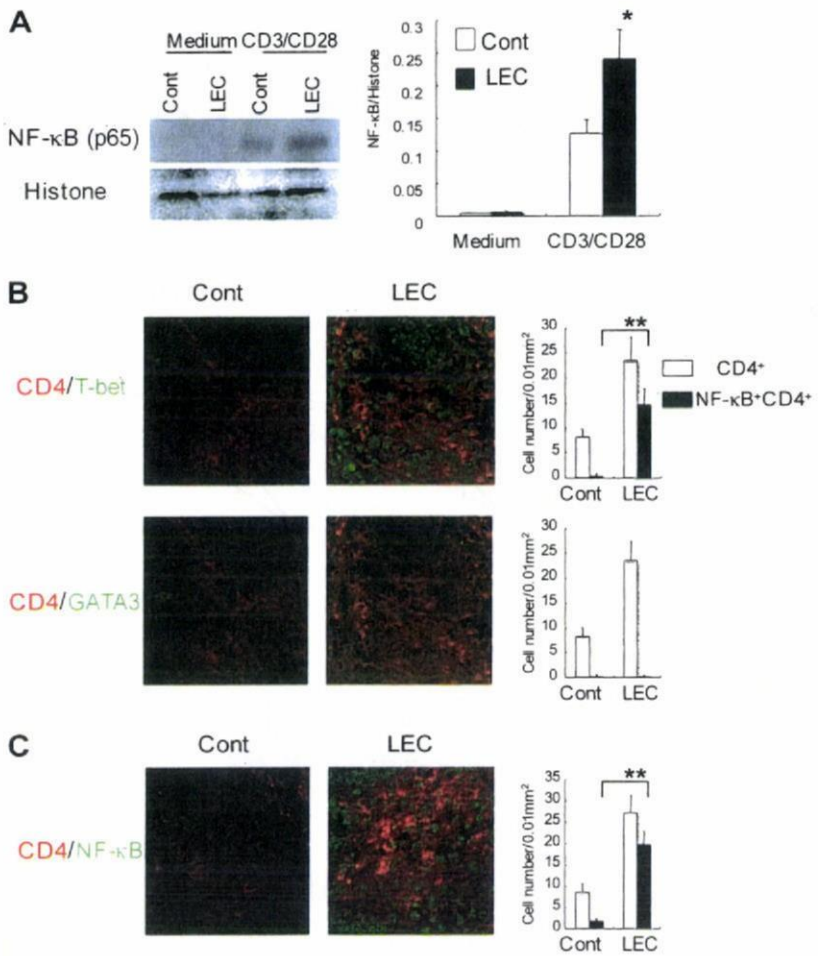

FIGURE 4. NF-κB activation of T cells in the IBD-like lesions from LEC rats. *A*, NF-κB activation of T cells from LEC rats. Purified MLN T cells were stimulated with CD3-CD28 ligation for 24 h, and the expressions of NF-κB (p65) and histone as a housekeeping protein in the nuclear extracts were tested by Western blotting. Relative expression of NF-κB to histone was calculated. Photos are representative and data are mean ± SD of three independent experiments. *B* and *C*, Confocal analysis of T-bet, GATA-3, and NF-κB of infiltrating $CD4^+$ T cells in IBD-like lesions from LEC and control rats. Frozen sections were stained with Alexa 488-labeled T-bet, GATA-3, or NF-κB (green), and Alexa 568-labeled CD4 (red). Photos are shown as representative of three samples. Data are mean ± SD of cell number ($CD4^+$ or $NF\text{-}\kappa B^+CD4^+$) per 0.01 mm^2 of five independent areas. **, $p < 0.005$ control vs LEC rats.

of MLNs and LP from LEC rats were significantly increased compared with those from control rats (Fig. 2*C*). As for CD69 expression, one of early activation markers, there was no difference between control and LEC rats (data not shown). These findings strongly suggest that $CD4^+$ T cells of MLNs and LP from LEC rats may play a crucial role in the development of spontaneous IBD-like lesions of LEC rats.

We next analyzed the proliferative response of T cells from LEC and control rats using stimulation with anti-CD3 and -CD28 mAbs. Purified T cells from spleen and MLNs of LEC and control rats were stimulated with plate-coated anti-CD3 mAb (0~1 μg/ml) and anti-CD28 mAb (5 μg/ml) for 72 h. It was previously reported that splenic T cell response to Con A of LEC rats was significantly reduced (32). Consistent with the report, the proliferative responses of splenic T cells with CD3-CD28 ligation were significantly lower than that from control rats (Fig. 2*D*). However, it was interesting to note that a prominent increase in T cell response with CD3-CD28 ligation in MLNs from LEC rats was observed compared with that from control rats (Fig. 2*D*). To clarify which population of T cells indicates higher proliferative response, the purified T cells of MLNs were labeled with CFSE, and stimulated with CD3-CD28 ligation for 72 h. Proliferative response of $CD4^+$ or $CD8^+$ T cells was analyzed by flow cytometry using CFSE dilutions. We found that $CD4^+$ T cells of MLNs from LEC rats were clearly much more proliferative compared with those from control rats, whereas no difference was observed in $CD8^+$ T cells between LEC and control rats (Fig. 2*E*). These results indicate that the $CD4^+$ T cells in MLNs from LEC rats are primarily responsible for the development of IBD-like lesions in LEC rats.

Cytokine switching of T cells in LEC rats

To define the function of T cells of spleen and MLNs from LEC rats, cytokine production in the culture supernatants from T cells stimulated with CD3-CD28 ligation was analyzed. IL-2 production in the spleen cells from LEC rats was significantly lower (anti-CD3 mAb: 0.5 and 1 μg/ml) than those in control rats (Fig. 3*A*). As for IFN-γ in spleen, no difference was observed between LEC and control rats. In addition, a significant decrease in Th2 cytokine production including IL-4 and IL-10 was observed in the spleen cells from LEC rats. In contrast, Th1 cytokines (IL-2 and IFN-γ) in the T cells of MLNs from LEC rats were significantly increased compared with those in control rats (Fig. 3*A*). By contrast, IL-10 production from MLN T cells in LEC rats was significantly lower (anti-CD3 mAb: 1 μg/ml) than that in control rats. No difference in IL-4 production between LEC and control rats was observed. These results indicate that the Th1 response of MLN T cells from LEC rats may influence the pathogenesis of IBD-like lesions in LEC rats.

It is well known that T-bet and GATA-3 are key transcription factors in controlling Th1 or Th2 cytokine production (4, 5). We then analyzed the expression T-bet and GATA-3 using the T cells of MLNs stimulated with CD3-CD28 ligation. T-bet expression of T cells from LEC rats was relatively increased comparing with that from control rats, whereas no difference in GATA-3 expression was observed between LEC and control rats (Fig. 3*B*). Moreover, the expression of STAT-1 and STAT-6, which exist upstream of T-bet and GATA-3, respectively, was analyzed. Increased phosphorylation of STAT-1 in T cells of MLNs from LEC rats was

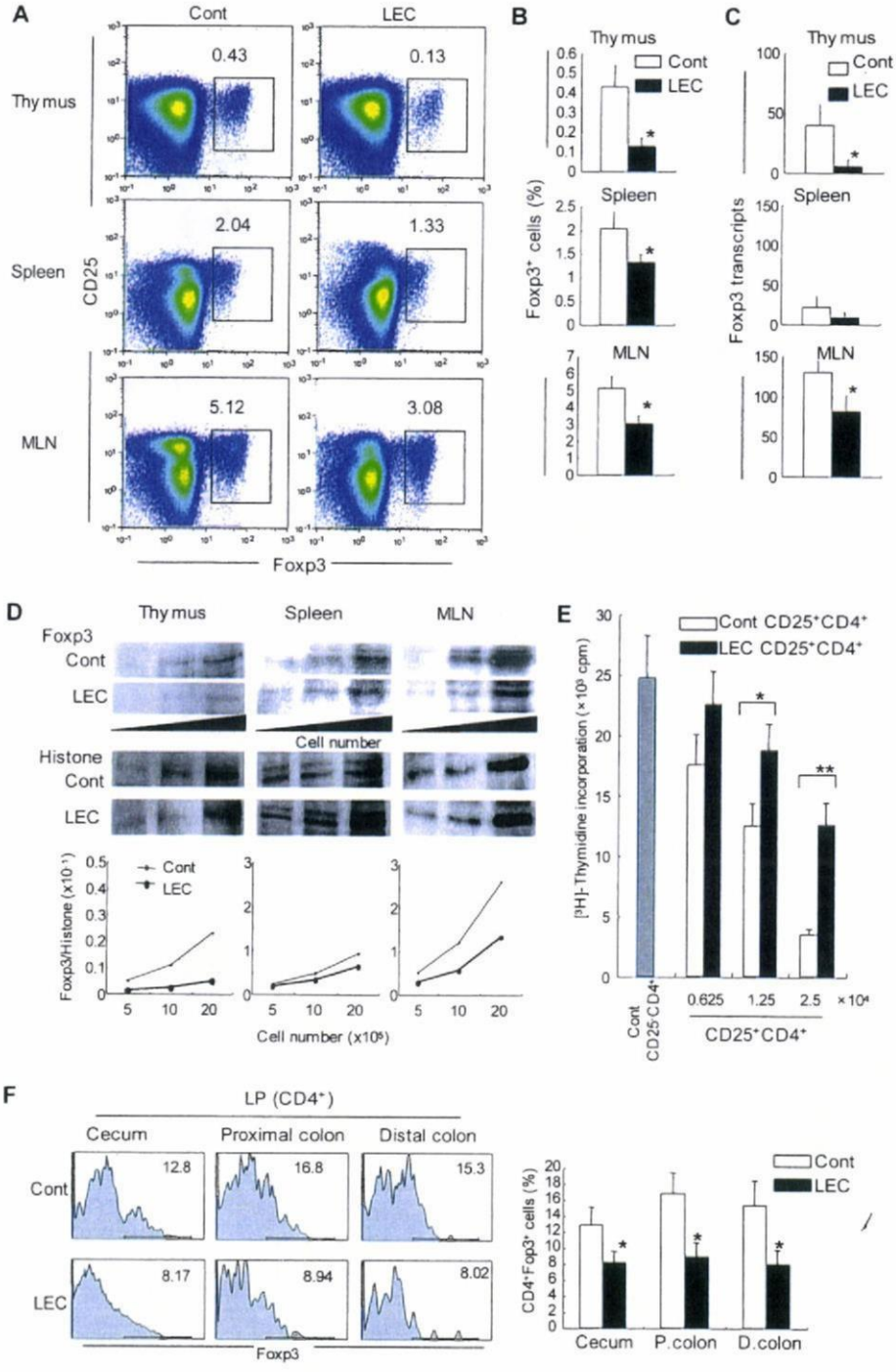

FIGURE 5. $CD25^+Foxp3^+CD4^+$ T cells in LEC rats. *A*, $CD25^+Foxp3^+CD4^+$ T cells in the thymus, spleen, and MLNs from LEC and control rats were analyzed by flow cytometry. Graphs are representative of three samples. *B*, $CD25^+Foxp3^+CD4^+$ T cells (percent) were shown as mean ± SD of three samples. *, $p < 0.05$; **, $p < 0.005$; ***, $p < 0.0005$ LEC vs control rats. *C*, The mRNA expression of Foxp3 in LEC rats. The expressions of the thymus, spleen, and MLNs were tested by real-time quantitative RT-PCR. Relative Foxp3 transcripts to HPRT were shown as mean ± SD of three samples. *, $p < 0.05$ LEC vs control rats. *D*, The Foxp3 expression of the nuclear extracts of 0.5×10^6, 1×10^6, and 2×10^6 $CD4^+$ T cells was confirmed by Western blotting. Histone was used as a housekeeping protein. Protein quantification of Foxp3 was performed using chemiluminescence images. Relative Foxp3 expression to histone of the nuclear extracts of 0.5×10^6, 1×10^6, and 2×10^6 T cells was estimated. Results are representative of three samples. *E*, A total of 5×10^4 $CD25^-CD4^+$ T cells of MLN from control rats were cocultured with 0.625–2.5 $\times 10^4$ $CD25^+CD4^+$ T cells of MLNs from control or LEC rats on anti-CD3 mAb-coated plate. Data are mean ± SD of triplicates, representative of three independent experiments. *, $p < 0.05$; **, $p < 0.005$ control $CD25^+CD4^+$ vs LEC $CD25^+CD4^+$. *F*, Foxp3 expression of $CD4^+$ LPMCs in cecum, proximal, and distal colon from control and LEC rats was detected. Results are representative of four to six rats. Data are mean ± SD of $CD4^+Foxp3^+$ cells (percent) of four to six rats. *, $p < 0.05$ control vs LEC rats.

detected, but no difference was observed in STAT-1 expression between LEC and control rats. By contrast, there was no difference in the expression and phosphorylation of STAT-6 in either group (Fig. 3*B*). To quantify the protein expressions of T-bet, pStat-1, GATA-3, and pSTAT-6, relative expressions to GAPDH as a housekeeping protein were shown in Fig. 3*C*. T-bet expression of stimulated MLN T cells from LEC rats was 4~5-fold higher compared with that of control rats. The pSTAT-1 had an expression that was twice as high relative to that of control rats. Furthermore, increased expression of Th1 cytokines including IL-2 and IFN-γ of $CD4^+$ T cells in LP from LEC rats was observed compared with that from control rats by fluorescence staining (Fig. 3*D*). By contrast, IL-4- or IL-10-producing cells were undetectable in the LP from both control and LEC rats (data not shown). To examine the correlation of Th1 cytokine with colitis of LEC rats, anti-IFN-γ-neutralizing Ab, anti-IL-4-neutralizing Ab, or isotype control Ab was injected into LEC rats from 8 to 10 wk of age, and the histology of colitis was evaluated (Fig. 3*E*). Histological score of LEC rats administrated with anti-IFN-γ mAb was significantly lower than that with isotype control Ab. No significant change was observed by injection of anti-IL-4 mAb. Moreover, to investigate the role of $CD8^+$ T cells in the development of colitis, anti-CD8-neutralizing Ab to deplete $CD8^+$ T cells was injected into LEC rats. There was no significant change of pathology in anti-CD8 mAb administered LEC rats, compared with that in controls (Fig. 3*E*). Ulcer formation, lymphocyte infiltrates, decreased numbers of mucin-producing cells, and mucosal hyperplasia were observed in the sections from isotype control Ab, anti-IL-4 mAb, and anti-CD8 mAb-injected rats, while injection of anti-IFN-γ mAb was able to effectively suppress the colon lesion of LEC rats (Fig. 3, *E* and *F*).

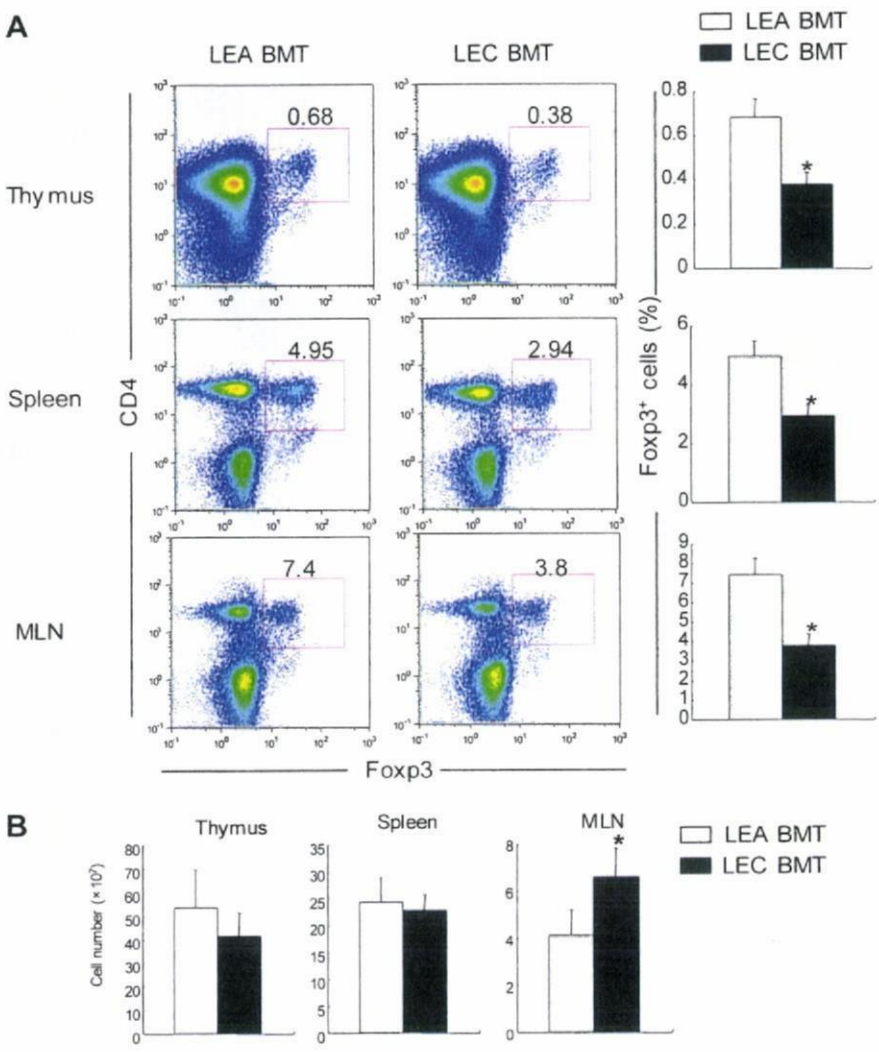

FIGURE 6. *A*, The generation of Treg cells from BM cells in LEC rats. A total of 5×10^6 BM cells from LEA or LEC rats were i.v. transferred into irradiated (4 Gy) LEA rats. At 4 wk after transfer, intracellular Foxp3 expression of $CD4^+CD25^+$ cells in thymus, spleen, and MLNs from the chimeric rats were analyzed by flow cytometry. Results are representative of three mice, and data are shown as the mean ± SD of three rats. *, $p < 0.05$ LEA BMT vs LEC BMT recipients. *B*, Total cell number in thymus, spleen, and MLN from LEA BMT and LEC recipient rats were counted with trypan blue staining. Data are mean ± SD of three rats. *, $p < 0.05$ LEA BMT vs LEC BMT.

NF-κB activation of T cells in IBD-like lesions from LEC rats

To further confirm whether the T cell signal via up-regulated T-bet and phosphorylation STAT-1 in MLN T cells from LEC rats can lead to NF-κB activation, which is a potent transcription factor regulating the target genes essential for T cell activation or proliferation (38–41), we analyzed NF-κB expression of the nuclear extracts of T cells stimulated with CD3-CD28 ligation. We demonstrated that there was an increased nuclear translocation of NF-κB (p65) of stimulated T cells in LEC rats compared with that in control rats (Fig. 4*A*).

We next examined the expression of T-bet, GATA-3, and nuclear translocation of NF-κB of infiltrating $CD4^+$ T cells in IBD-like lesions from LEC rats by confocal microscopy. Increased expression of T-bet together with nuclear transport of NF-κB was observed in $CD4^+$ T cells of inflammatory lesions from LEC rats (Fig. 4, *B* and *C*), whereas GATA-3^+ $CD4^+$ T cells were almost undetectable in the lesions (Fig. 4*B*). These results imply that T cells of LEC rats might be activated as effecter cells through STAT-1, T-bet, and NF-κB, resulting in Th1 cytokine production which affect the development of IBD-like lesions of LEC rats.

Treg cells in LEC rats

It has been reported that regulatory immune cells such as $CD4^+CD25^+$ T cells play a crucial role for the pathogenesis of both human IBD and the animal models (21, 22, 24). Thus, we analyzed whether $CD4^+CD25^+$ regulatory T cells influence the development of IBD-like lesions via the immune disorder of LEC rats. First, the cell populations of $CD4^+CD25^+$ T cells in the thymus, spleen, and MLNs form control and LEC rats were analyzed by flow cytometry. $CD4^+CD25^+$ T cells are known to express high levels of Foxp3, a transcription factor that in a normal rat is selectively expressed in $CD25^+$ Treg cells (20). The number of $CD25^+Foxp3^+$ Treg cells of the thymus, spleen, and MLN from LEC rats was significantly lower than that of control rats (Fig. 5, *A* and *B*). In particular, Treg cells of the thymus and MLNs from LEC rats were reduced in contrast to control rats (thymus; $p = 0.0113$, MLN; $p = 0.0133$). Moreover, $Foxp3^+CD4^+$ T cells in MLN from LEC rats were significantly reduced relative to that from control rats (Fig. 5*B*). Interestingly, $Foxp3^+$ Tregs in MLNs (5.12 ± 0.71%) from control rats were markedly increased relative to that in the thymus (0.43 ± 0.11%) and spleen (2.04 ± 0.34%) as shown in Fig. 5*B*. We next assessed the mRNA expression of Foxp3 in the thymus, spleen, and MLNs from LEC and control rats using real-time quantitative RT-PCR. Consistent with the results of flow cytometric analysis (Fig. 5, *A* and *B*), mRNA expression of Foxp3 in the thymus and MLNs from LEC rats was significantly reduced relative to that from control rats (Fig. 5*C*). The prominent expression of Foxp3 mRNA in MLNs from both LEC and control rats was observed comparing with that of the thymus and spleen from both groups (Fig. 5*C*). Furthermore, we confirmed the protein levels of Foxp3 using the nuclear extracts of $CD4^+$ T cell in the thymus, spleen, and MLNs from LEC and control rats by Western

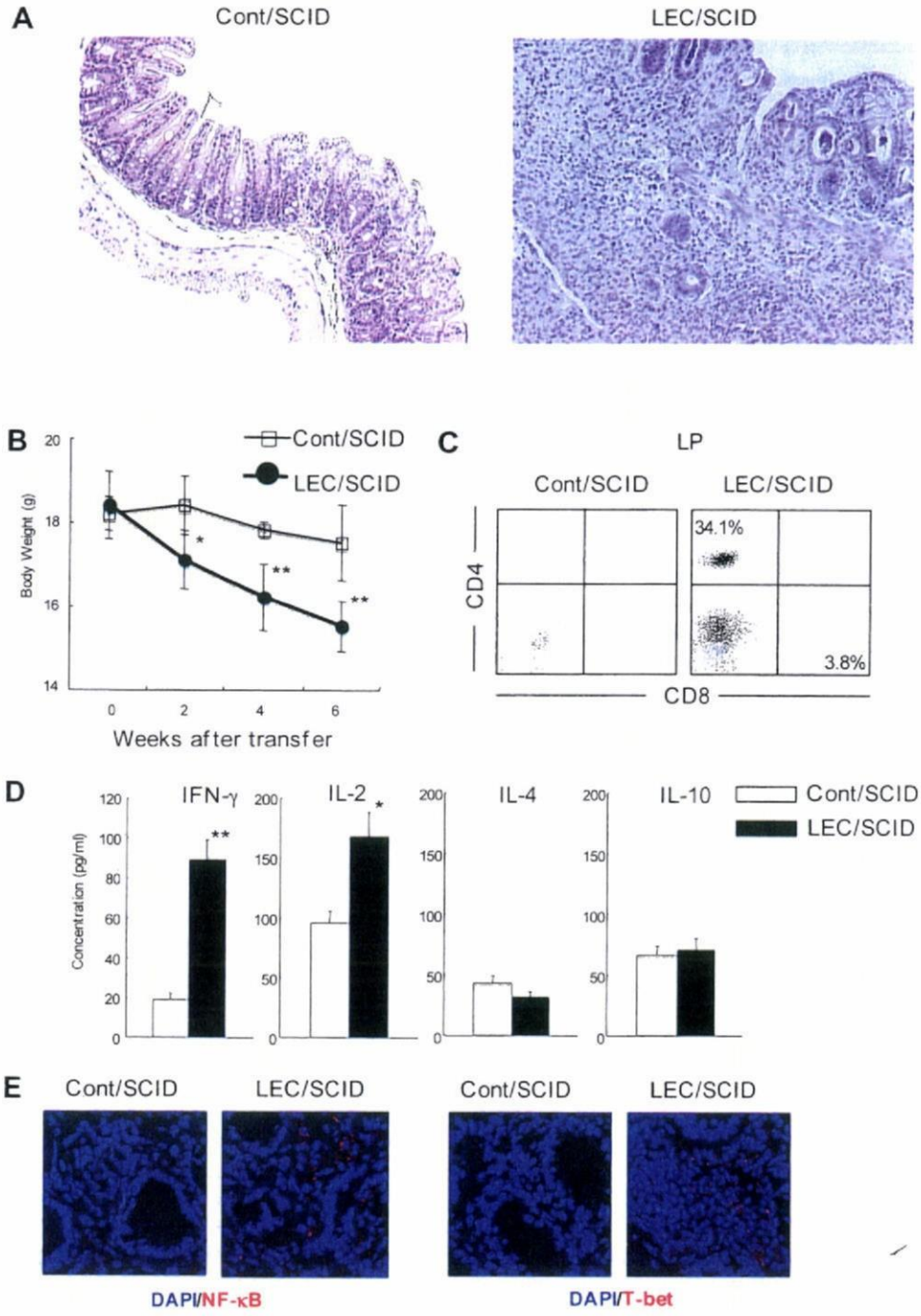

FIGURE 7. Transferable lesions of LEC rats into SCID mice. The pooled MLN T cells (5×10^6) from LEC and control rats were transferred i.p. into SCID mice as recipients. The SCID mice were analyzed at 6 wk after transfer. *A*, Induction of colon lesions in recipient SCID mice. Representative photomicrographs (original magnification, ×100) of H&E-stained paraffin sections of colon from Cont/SCID and LEC/SCID recipients were shown. *B*, The change of body weight of Cont/SCID- and LEC/SCID-recipient mice. After transfer body weight of recipient mice was monitored once in 2 wk. The data are shown as the mean ± SD of approximately four to eight mice. *, $p < 0.05$; **, $p < 0.005$ LEC vs control rats. *C*, Infiltrating T cells in the colon tissues of recipient mice. Purified lymphocytes from the LP in colon of recipient mice were stained with PE-conjugated CD4 mAb and FITC-conjugated CD8 mAb, and analyzed by flow cytometry. Figures were representative of approximately four to eight samples. *D*, Th1-shifted cytokine pattern of LEC/SCID recipients. The supernatants from MLN cells stimulated with CD3-CD28 ligation for 24 h were used to detect the concentration of cytokine productions by ELISA. The data are shown as the mean ± SD of triplicate samples. *, $p < 0.05$; **, $p < 0.005$ LEC/SCID vs Cont/SCID recipients. *E*, NF-κB and T-bet expressions of LPMCs colon were detected by staining with the first mAbs, Alexa 568-conjugated anti-mouse IgG as the second Ab, and DAPI. Photos are representative of three samples.

blotting. As expected, the protein expression of Foxp3 in the thymus and MLNs from LEC rats was markedly lower, and its expression in the spleen from LEC was slightly decreased, compared with the control rats (Fig. 5*D*). Moreover, to clarify the function of Treg cells from LEC rats, T cell suppression assay was performed. Namely, $CD25^-CD4^+$ T cells from control rats were stimulated with plate-coated anti-CD3 mAb and cocultured with control or LEC Treg cells. Although control Treg cells suppressed T cell response considerably, the suppressive function of LEC Treg cells was significantly impaired (Fig. 5*E*). In addition, when $Foxp3^+$ Treg cells in the each segment of colon including cecum, proximal, and distal colon were analyzed, $Foxp3^+$ cells of LPMCs from all segments in LEC rats were significantly decreased compared with those in control rats (Fig. 5*F*). These findings suggest that the decreased $CD4^+CD25^+Foxp3^+$ Tregs in the thymus, MLNs, and LPMCs might affect the intestinal immunity associated with IBD-like lesions in LEC rats.

Treg cells from bone marrow (BM) cells of LEC rats

To know whether the decreased number of Treg cells in LEC rats is derived from the BM cells or not, the BM cells from LEA or LEC rats were transferred into irradiated LEA rats. The number of $Foxp3^+CD25^+CD4^+$ Treg cells in thymus, spleen, and MLNs of chimeric rats was analyzed by flow cytometry. In parallel with the decreased numbers of Treg cells from LEC rats, the $Foxp3^+$ Treg cells of thymus, spleen, and MLNs in the chimeric rats transferred with LEC BM cells were significantly reduced compared with those from LEA BM cells (Fig. 6*A*). Moreover, as to the expansion of T cells from BM cells, although thymocytes and spleen cells of LEC BM cell transplantation (BMT) rats were slightly decreased

Table I. *Induction of IBD-like lesions of LEC rats into SCID mice*

Transfer[a]	Incidence %[b]	Induction/Total
SCID control	0	0/5
Cont/spleen→SCID	0	0/4
LEC/spleen→SCID	0	0/4
Cont/MLN→SCID	0	0/7
LEC/MLN→SCID	87.5	7/8

[a] Purified T cells of MLN or spleen from LEC and control rats were transferred into SCID mice. Six weeks later, histological analysis of colon lesions from SCID recipients was performed.
[b] Incidence of IBD-like lesions was evaluated using four to eight SCID recipients.

compared with those of LEA BMT rats, a significantly increased cell number of MLN from LEC BMT rats was observed (Fig. 6*B*). These findings indicate that the precursor of Treg may exist in the BM, and that the generation of Treg precursors in LEC rats might be deficient in the BM in addition to the deficiency of thymic differentiation.

Induction of IBD-like lesions by adoptive transfer of MLN T cells from LEC rats into SCID mice

To determine whether inflammatory bowel lesions of LEC rats could be induced in SCID mice via a T cell-mediated pathway, adoptive transfer of T cells in MLNs from LEC rats into SCID mice was performed. Importantly, inflammatory lesions of transferred SCID mice with MLN T cells were observed restrictedly in the colon, while no lesion was detected in Cont/SCID recipients at this stage (Fig. 7*A* and Table I). In addition to the IBD-like lesions, the body weight of LEC/SCID recipients transferred with MLN T cells from LEC rats was significantly decreased after the transfer compared with that from Cont/SCID recipients (Fig. 7*B*), whereas there was no change for Cont/SCID recipients. By contrast, adoptive transfer of splenic T cells from LEC rats did not induce any lesions in the SCID recipient (Table I). A large number of $CD4^+$ T cell population was observed within the infiltrating T cells from IBD-like lesions in IBD/SCID recipients (Fig. 7*C*). Moreover, it was demonstrated that MLN T cells stimulated with CD3 and CD28 from LEC/SCID recipients could produce higher levels of IL-2 and IFN-γ, not IL-4 and IL-10, than those from Cont/SCID recipients (Fig. 7*D*). Furthermore, the increased expressions of NF-κB and T-bet in LPMCs from LEC/SCID mice were detected compared with those from Cont/SCID mice (Fig. 7*E*). These results indicate that the IBD-like lesions of LEC rats can be transferred with MLN T cells, not splenic T cells, into SCID mice, and that Th1 response may play a pivotal role in the pathogenesis of IBD-like lesions in LEC rats.

Discussion

As for the animal models of IBD, there have been two categories reported previously (1). One is a spontaneous IBD model with any immune dysfunction such as in IL-$2^{-/-}$, IL-$2R^{-/-}$, IL-$10^{-/-}$, and $NOD2^{-/-}$ mice (18, 41–43). The other is a model manipulated by any drug, bacteria, and cell transfer (44–48). In this study, we demonstrated that the LEC rat is one of spontaneous IBD models, by which the mechanism is due to the decline of Treg cells and the Th1 shift of the cytokine.

T lymphocytes play a central role for the intestinal immune system (12, 49). Recent studies suggested that the balance between Th1 and Th2 cytokines secreted by T cells appears to regulate IBD (13, 39, 48). In this study, the pattern of cytokine production of MLN cells and LPMCs, but not spleen cells, in LEC rats had clearly shifted to Th1. It was reported that the proliferative response of peripheral T cells in LEC rats against T cell mitogen such as Con A had decreased, and that IL-2 production of T cells in LEC rats had reduced (32). However, we found here that proliferative response and Th1 cytokine production of MLN T cells through the TCR/CD3 and CD28 pathway had increased compared with that of control rats. The response of MLN T cells or LPMCs which may regulate the intestinal immune system seems to be different from that of spleen cells from a point of view of cytokine production, and any other immune functions. Namely, MLNs and LPMCs have unique functions regulating the intestinal immune system with exposure to numerous food, bacterial, and/or endogenous Ags. It is possible that defective thymic selection for differentiation into CD4SP cells form DP cells in LEC rats might influence any function including cytokine production in the peripheral T cells. It is well known that cytokine production of immune cells can be occurred through various stimuli such as microorganisms, inflammations, and mechanical or physiological stresses (45, 50–52). The balance between Th1 and Th2 cytokine production is controlled by a number of transcriptional factors and signaling molecules (4). Recent studies indicated that GATA-3 and T-bet might play a central role in controlling the balance of cytokine production from Th cells (4–7). We demonstrated here that Th1 response in MLN T cells and LPMCs through T-bet, STAT-1, and NF-κB might be considerably enhanced, and then the T cell response to numerous intestinal Ags could be responsible for the development of IBD-like lesions in LEC rats.

$CD4^+CD25^+Foxp3^+$ Treg cells have been widely investigated to be generated from the thymus and regulate the peripheral T cells (20). The defective thymic selection of LEC rat influences positive selection into $CD4^+$ from $CD4^+CD8^+$ cells, and results in the dysfunction of peripheral $CD4^+$ T cells (32). It has been reported that Treg cells can prevent IBD-like lesions induced by naive $CD4^+$ T cell transfer into T cell-deficient mice, and regulate Th1 effectors producing IFN-γ (24). In this study, it is speculated that the dysfunction of Treg cells in LEC rats might be associated with the hyperactivation of Th1 effectors in the periphery. In particular, Treg cells in MLNs and LPMCs might play a crucial role for regulating the immune response against numerous intestinal Ags. Therefore, the dysfunction of Treg cells in MLNs and LPMCs would be associated with the deficiency of intestinal tolerance, resulting in the development of IBD-like lesions in LEC rats. In contrast, although $Foxp3^+CD25^-$T cells were reported to have suppressive functions similar to those of $Foxp3^+CD25^+$ classical Treg cells in normal mice (53), there was no difference in the $Foxp3^+CD25^-$T cells (percent) of thymus (control; 0.063 ± 0.011%, LEC; 0.068 ± 0.018%), spleen (control; 0.25 ± 0.04%, LEC; 0.20 ± 0.06%), MLNs (control; 0.47 ± 0.07%, LEC; 0.41 ± 0.06%) between control and LEC rats. The $Foxp3^+CD25^+$ Treg cells, but not $Foxp3^+CD25^-$T cells, of LEC rats might influence the development of colitis of LEC rats.

Direct in vivo evidence of T cell-dependent IBD-like lesions of LEC rats is the induction of the lesion into SCID mice by adoptive transfer with MLN T cells from LEC rats. Although defective T cell functions have been previously reported using fetal thymus grafts of LEC rats into SCID mice, the inflammatory lesions in general have not been investigated (54). Although it is not unclear whether the precursor of Treg cell is generated in BM, the experiment using BM chimera of LEC and LEA rats may imply the origin of the Treg precursor in BM cells.

The LEC rat has been also reported to be used as an animal model for Wilson's disease and developed hepatitis from four months after birth because of the genetic copper metabolism disorder. At a later age, chronic hepatitis and hepatocellular carcinoma are observed in LEC rats (36, 55). The LEC rats have been useful in studying mechanisms of spontaneous carcinogenesis.

Generally described, it has been shown that the pathogenesis of colon cancer could be associated with chronic inflammation such as IBD (56). Previous studies demonstrated that there was a high frequency of 7 *N*-methyl-*N*-nitrosourea-induced colon adenocarcinoma in LEC rats was observed compared with that of control rats (57). It can be speculated that IBD-like inflammatory lesions of LEC rats might affect the carcinogenesis via any indirect mechanism. Although LEC rats were described to have the defective differentiation of CD4 SP cells in the thymus, the decline of peripheral $CD4^+$ T cells, and the failure of proliferative response to T cell mitogen in $CD4^+$ T cells, any inflammatory disease based on these immune disorders has not been investigated. In contrast, the mutation of Th immunodeficiency (*thid*) gene was previously reported (58), which might be associated with immune disorder of LEC rats. Our study focused on Treg cells and cytokine switching as the mechanisms of IBD-like lesions of LEC rats. It is still unclear whether *thid* gene regulates the generation of Treg cells and cytokine switching through T-bet and STAT-1 leading to NF-κB in $CD4^+$ T cells from LEC rats.

In summary, we demonstrated for the first time that IBD-like lesions developed spontaneously in LEC rats. The dysfunction of Treg cells in the periphery and Th1 shift of cytokine production might play a crucial role for pathogenesis of IBD-like lesions in LEC rats. Analyzing the molecular mechanism for IBD-like lesions in LEC rats will be useful for understanding human IBD based on immune disorder in central and peripheral tolerance.

Acknowledgments

We thank Ai Nagaoka and Satoko Yoshida for their technical assistance.

Disclosures

The authors have no financial conflict of interest.

References

1. Blumberg, R. S., L. J. Saubermann, and W. Strober. 1999. Animal models of mucosal inflammation and their relation to human inflammatory bowel disease. *Curr. Opin. Immunol.* 11: 648–656.
2. Fiocchi, C. 1998. Inflammatory bowel disease: etiology and pathogenesis. *Gastroenterology* 115: 182–205.
3. Fiocchi, C. 2005. Inflammatory bowel disease pathogenesis: therapeutic implications. *Chin. J. Dig. Dis.* 6: 6–9.
4. Rengarajan, J., S. J. Szabo, and L. H. Glimcher. 2000. Transcriptional regulation of Th1/Th2 polarization. *Immunol. Today* 21: 479–483.
5. Zheng, W., and R. A. Flavell. 1997. The transcription factor GATA-3 is necessary and sufficient for Th2 cytokine gene expression in CD4 T cells. *Cell* 89: 587–596.
6. Asnagli, H., and K. M. Murphy. 2001. Stability and commitment in T helper cell development. *Curr. Opin. Immunol.* 13: 242–247.
7. Neurath, M. F., B. Weigmann, S. Finotto, J. Glickman, E. Nieuwenhuis, H. Iijima, A. Mizoguchi, E. Mizoguchi, J. Mudter, P. R. Galle, et al. 2002. The transcription factor T-bet regulates mucosal T cell activation in experimental colitis and Crohn's disease. *J. Exp. Med.* 195: 1129–1143.
8. Strober, W., I. J. Fuss, and R. S. Blumberg. 2002. The immunology of mucosal models of inflammation. *Annu. Rev. Immunol.* 20: 495–549.
9. Neurath, M. F., S. Finotto, I. J. Fuss, M. Boirivant, P. R. Galle, and W. Strober. 2001. Regulation of T-cell apoptosis in inflammatory bowel disease: to die or not to die, that is the mucosal question. *Trends Immunol.* 22: 21–26.
10. Atreya, R., J. Mudter, S. Finotto, J. Mullberg, T. Jostock, S. Wirtz, M. Schutz, B. Bartsch, M. Holtmann, C. Becker, et al. 2000. Blockade of interleukin 6 trans signaling suppresses T-cell resistance against apoptosis in chronic intestinal inflammation: evidence in Crohn disease and experimental colitis in vivo. *Nat. Med.* 6: 583–588.
11. Plevy, S. E., C. J. Landers, J. Prehn, N. M. Carramanzana, R. L. Deem, D. Shealy, and S. R. Targan. 1997. A role for TNF-α and mucosal T helper-1 cytokines in the pathogenesis of Crohn's disease. *J. Immunol.* 159: 6276–6282.
12. Iijima, H., M. F. Neurath, T. Nagaishi, J. N. Glickman, E. E. Nieuwenhuis, A. Nakajima, D. Chen, I. J. Fuss, N. Utku, D. N. Lewicki, et al. 2004. Specific regulation of T helper cell 1-mediated murine colitis by CEACAM1. *J. Exp. Med.* 199: 471–482.
13. Fuss, I. J., M. Neurath, M. Boirivant, J. S. Klein, C. de la Motte, S. A. Strong, C. Fiocchi, and W. Strober. 1996. Disparate $CD4^+$ lamina propria (LP) lymphokine secretion profiles in inflammatory bowel disease: Crohn's disease LP cells manifest increased secretion of IFN-γ, whereas ulcerative colitis LP cells manifest increased secretion of IL-5. *J. Immunol.* 157: 1261–1270.
14. Neurath, M. F., I. J. Fuss, B. L. Kelsall, D. H. Presky, W. Waegell, and W. Strober. 1996. Experimental granulomatous colitis in mice is abrogated by induction of TGF-β-mediated oral tolerance. *J. Exp. Med.* 183: 2605–2616.
15. Kitani, A., I. J. Fuss, K. Nakamura, O. M. Schwartz, T. Usui, and W. Strober. 2000. Treatment of experimental (Trinitrobensene sulfonic acid) colitis by intranasal administration of transforming growth factor (TGF)-β1 plasmid: TGF-β1-mediated suppression of T helper cell type 1 response occurs by interleukin (IL)-10 induction and IL-12 receptor β2 chain downregulation. *J. Exp. Med.* 195: 41–52.
16. Eckmann, L., and M. Karin. 2005. NOD2 and Crohn's disease: loss or gain of function? *Immunity* 22: 661–667.
17. Girardin, S. E., J. P. Hugot, and P. J. Sansonetti. 2003. Lessons from Nod2 studies: towards a link between Crohn's disease and bacterial sensing. *Trends Immunol.* 24: 652–658.
18. Murray, P. J. 2005. NOD proteins: an intracellular pathogen-recognition system or signal transduction modifiers? *Curr. Opin. Immunol.* 17: 352–358.
19. Watanabe, T., A. Kitani, P. J. Murray, and W. Strober. 2004. NOD2 is a negative regulator of Toll-like receptor 2-mediated T helper type 1 responses. *Nat. Immunol.* 5: 800–808.
20. Sakaguchi, S. 2005. Naturally arising Foxp3-expressing $CD25^+CD4^+$ regulatory T cells in immunological tolerance to self and non-self. *Nat. Immunol.* 6: 345–352.
21. Maul, J., C. Loddenkemper, P. Mundt, E. Berg, T. Giese, A. Stallmach, M. Zeitz, and R. Duchmann. 2005. Peripheral and intestinal regulatory $CD4^+$ $CD25^{high}$ T cells in inflammatory bowel disease. *Gastroenterology* 128: 1868–1878.
22. Fantini, M. C., C. Becker, I. Tubbe, A. Nikolaev, H. A. Lehr, P. R. Galle, and M. F. Neurath. 2005. TGF-β induced $Foxp3^+$ regulatory T cells suppress Th1-mediated experimental colitis. *Gut* 55: 671–680.
23. Singh, B., S. Read, C. Asseman, V. Malmstrom, C. Mottet, L. A. Stephens, R. Stepankova, H. Tlaskalova, and F. Powrie. 2001. Control of intestinal inflammation by regulatory T cells. *Immunol. Rev.* 182: 190–200.
24. Martin, B., A. Banz, B. Bienvenu, C. Cordier, N. Dautigny, C. Becourt, and B. Lucas. 2004. Suppression of $CD4^+$ T lymphocyte effector functions by $CD4^+CD25^+$ cells in vivo. *J. Immunol.* 172: 3391–3398.
25. Niederau, C., F. Backmerhoff, B. Schumacher, and C. Niederau. 1997. Inflammatory mediators and acute phase proteins in patients with Crohn's disease and ulcerative colitis. *Hepatogastroenterology* 44: 90–107.
26. Nielsen, O. H., T. Ciardelli, Z. Wu, E. Langholz, and I. Kirman. 1995. Circulating soluble interleukin-2 receptor α and β chain in inflammatory bowel disease. *Am. J. Gastroenterol.* 90: 1301–1306.
27. Poussier, P., T. Ning, J. Chen, D. Banerjee, and M. Julius. 2000. Intestinal inflammation observed in IL-2R/IL-2 mutant mice is associated with impaired intestinal T lymphopoiesis. *Gastroenterology* 118: 880–891.
28. Sohn, K. J., S. A. Shah, S. Reid, M. Choi, J. Carrier, M. Comiskey, C. Terhorst, and Y. I. Kim. 2001. Molecular genetics of ulcerative colitis-associated colon cancer in the interleukin 2- and β_2-microglobulin-deficient mouse. *Cancer Res.* 61: 6912–6917.
29. El Yousfi, M., M. D. Breuille, I. Papet, S. Blum, M. Andre, L. Mosoni, P. Denis, C. Buffiere, and C. Obled. 2003. Increased tissue protein synthesis during spontaneous inflammatory bowel disease in HLA-B27 rats. *Clin. Sci. Lond.* 105: 437–446.
30. Elson, C. O., Y. Cong, V. J. McCracken, R. A. Dimmitt, R. G. Lorenz, and C. T. Weaver. 2005. Experimental models of inflammatory bowel disease reveal innate, adaptive, and regulatory mechanisms of host dialogue with the microbiota. *Immunol. Rev.* 206: 260–276.
31. Davidson, N. J., M. W. Leach, M. M. Fort, L. Thompson-Snipes, R. Kuhn, W. Muller, D. J. Berg, and D. M. Rennick. 1996. T helper cell 1-type $CD4^+$ T cells, but not B cells, mediate colitis in interleukin 10-deficient mice. *J. Exp. Med.* 184: 241–251.
32. Agui, T., M. Oka, Y. Yamada, T. Sakai, K. Izumi, Y. Ishida, K. Himeno, and K. Matsumoto. 1990. Maturational arrest from $CD4^+8^+$ to $CD4^+8^-$ thymocytes in a mutant strain (LEC) of rat. *J. Exp. Med.* 172: 1615–1624.
33. Sakai, T., T. Agui, K. Wei, M. Oka, H. Hisaeda, H. Nagasawa, K. Himeno, and K. Matsumoto. 1998. Unresponsiveness of $CD4^-8^{+/-}$ thymocytes to lectin stimulation in LEC mutant rats. *Immunology* 95: 219–225.
34. Collison, L. W., C. J. Workman, T. T. Kuo, K. Boyd, Y. Wang, K. M. Vignali, R. Cross, D. Sehy, R. S. Blumberg, and D. A. A. Vignali. 2007. The inhibitory cytokine IL-35 contributes to regulatory T-cell function. *Nature* 22: 566–571.
35. Xystrakis, E., A. S. Dejean, I. Bernard, P. Druet, R. Liblau, D. Gonzalez-Dunia, and A. Saoudi. 2004. Identification of a novel natural regulatory CD8 T-cell subset and analysis of its mechanism of regulation. *Blood* 104: 3294–3301.
36. Li, Y., Y. Togashi, S. Sato, T. Emoto, J. H. Kang, N. Takeichi, H. Kobayashi, Y. Kojima, Y. Une, and J. Uchida. 1991. Spontaneous hepatic copper accumulation in Long-Evans Cinnamon rats with hereditary hepatitis: a model of Wilson's disease. *J. Clin. Invest.* 87: 1858–1861.
37. Yamazaki, K., H. Ohyama, K. Kurata, and T. Wakabayashi. 1993. Effects of dietary vitamin E on clinical course and plasma glutamic oxaloacetic transaminase and glutamic pyruvic transaminase activities in hereditary hepatitis of LEC rats. *Lab. Anim. Sci.* 43: 61–67.
38. Das, J., C. H. Chen, L. Yang, L. Cohn, P. Ray, and A. Ray. 2001. A critical role for NF-κB in GATA3 expression and TH2 differentiation in allergic airway inflammation. *Nat. Immunol.* 2: 45–50.
39. Hwang, E. S., J. H. Hong, and L. H. Glimcher. 2005. IL-2 production in developing Th1 cells is regulated by heterodimerization of RelA and T-bet and requires T-bet serine residue 508. *J. Exp. Med.* 202: 1289–1300.
40. Torgerson, T. R., A. D. Colosia, J. P. Donahue, Y. Z. Lin, and J. Hawiger. 1998. Regulation of NF-κB, AP-1, NFAT, and STAT1 nuclear import in T lymphocytes

by noninvasive delivery of peptide carrying the nuclear localization sequence of NF-κB p50. *J. Immunol.* 161: 6084–6092.
41. Sadlack, B., H. Merz, H. Schorle, A. Schimpl, A. C. Feller, and I. Horak. 1993. Ulcerative colitis-like disease in mice with a disrupted interleukin-2 gene. *Cell* 75: 253–261.
42. Asseman, C., S. Mauze, M. W. Leach, R. L. Coffman, and F. Powrie. 1999. An essential role for interleukin 10 in the function of regulatory T cells that inhibit intestinal inflammation. *J. Exp. Med.* 190: 995–1004.
43. Eckmann, L. 2004. Innate immunity and mucosal bacterial interactions in the intestine. *Curr. Opin. Gastroenterol.* 20: 82–88.
44. Brimnes, J., J. Reimann, M. Nissen, and M. Claesson. 2001. Enteric bacterial antigens activate CD4$^+$ T cells from *scid* mice with inflammatory bowel disease. *Eur. J. Immunol.* 31: 23–31.
45. Kullberg, M. C., J. F. Andersen, P. L. Gorelick, P. Caspar, S. Suerbaum, J. G. Fox, A. W. Cheever, D. Jankovic, and A. Sher. 2003. Induction of colitis by a CD4$^+$ T cell clone specific for a bacterial epitope. *Proc. Natl. Acad. Sci. USA* 100: 15830–15835.
46. Aranda, R., B. C. Sydora, P. L. McAllister, S. W. Binder, H. Y. Yang, S. R. Targan, and M. Kronenberg. 1997. Analysis of intestinal lymphocytes in mouse colitis mediated by transfer of CD4$^+$, CD45RB^{high} T cells to SCID recipients. *J. Immunol.* 158: 3464–3473.
47. Powrie, F., M. W. Leach, S. Mauze, S. Menon, L. B. Caddle, and R. L. Coffman. 1994. Inhibition of Th1 responses prevents inflammatory bowel disease in *scid* mice reconstituted with CD45RB^{hi} CD4$^+$ T cells. *Immunity* 1: 553–562.
48. Kanai, T., T. Kawamura, T. Dohi, S. Makita, Y. Nemoto, T. Totsuka, and M. Watanabe. 2006. TH1/TH2-mediated colitis induced by adoptive transfer of CD4$^+$CD45RB^{high} T lymphocytes into nude mice. *Inflamm. Bowel. Dis.* 12: 89–99.
49. Breese, E., C. P. Braegger, C. J. Corrigan, J. A. Walker-Smith, and T. T. MacDonald. 1993. Interleukin-2- and interferon-γ-secreting T cells in normal and diseased human intestinal mucosa. *Immunology* 78: 127–131.
50. Lodes, M. J., Y. Cong, C. O. Elson, R. Mohamath, C. J. Landers, S. R. Targan, M. Fort, and R. M. Hershberg. 2004. Bacterial flagellin is a dominant antigen in Crohn disease. *J. Clin. Invest.* 113: 1296–1306.
51. Fiorucci, S., E. Antonelli, E. Distrutti, P. Del Soldato, R. J. Flower, M. J. Clark, A. Morelli, M. Perretti, and L. J. Ignarro. 2002. NCX-1015, a nitric-oxide derivative of prednisolone, enhances regulatory T cells in the lamina propria and protects against 2,4,6-trinitrobenzene sulfonic acid-induced colitis in mice. *Proc. Natl. Acad. Sci. USA* 99: 15770–15775.
52. Zhou, P., R. Borojevic, C. Streutker, D. Snider, H. Liang, and K. Croitoru. 2004. Expression of dual TCR on DO11.10 T cells allows for ovalbumin-induced oral tolerance to prevent T cell-mediated colitis directed against unrelated enteric bacterial antigens. *J. Immunol.* 172: 1515–1523.
53. Zelenay, S., T. L. Carvalho, I. Caramalho, M. F. M. Fontes, M. Rebelo, and J. Demengeot. 2005. Foxp$^+$CD25$^+$CD4 T cells constitute a reservoir of committed regulatory cells that regain CD25 expression upon homeostatic expansion. *Proc. Natl. Acad. Sci. USA* 102: 4091–4096.
54. Chai, J. G., T. Sakai, H. Hisaeda, H. Nagasawa, K. Yasutomo, A. Furukawa, H. Ishikawa, Y. Maekawa, H. Uehara, K. Izumi, et al. 1996. Development of functional rat-derived T cells in SCID mice engrafted with the fetal thymus of LEC rats which are defective in CD4$^+$ T cells. *Microbiol. Immunol.* 40: 659–664.
55. Choudhury, S., R. Zhang, K. Frenkel, T. Kawamori, F. L. Chung, and R. Roy. 2003. Evidence of alterations in base excision repair of oxidative DNA damage during spontaneous hepatocarcinogenesis in Long Evans Cinnamon rats. *Cancer Res.* 63: 7704–7707.
56. Itzkowitz, S. 2003. Colon carcinogenesis in inflammatory bowel disease: applying molecular genetics to clinical practice. *J. Clin. Gastroenterol.* 36: S70–S74; discussion S94-76.
57. Min, H., E. Kudo, A. Hino, K. Yoshimoto, H. Iwahana, M. Itakura, and K. Izumi. 1997. *p53* gene mutation in *N*-butyl-*N*-(4-hydroxybutyl)nitrosamine-induced urinary bladder tumors and *N*-methyl-*N*-nitrosourea-induced colon tumors of rats. *Cancer Lett.* 117: 81–86.
58. Wei, K., Y. Muramatsu, T. Sakai, T. Yamada, and K. Matsumoto. 1997. Chromosomal mapping of the T-helper immunodeficiency (*thid*) locus in LEC rats. *Immunogenetics* 47: 99–102.

Crosstalk between RANKL and Fas signaling in dendritic cells controls immune tolerance

Takashi Izawa,[1,2] Naozumi Ishimaru,[1] Keiji Moriyama,[2] Masayuki Kohashi,[1] Rieko Arakaki,[1] and Yoshio Hayashi[1]

[1]Department of Oral Molecular Pathology, Institute of Health Biosciences, The University of Tokushima Graduate School, Kuramotocho, Tokushima, Japan; [2]Department of Orthodontics and Dentofacial Orthopedics, Institute of Health Biosciences, The University of Tokushima Graduate School, Kuramotocho, Tokushima, Japan

Although receptor activator of nuclear factor (NF)–κB ligand (RANKL) signaling has been shown to prolong the survival of mature dendritic cells (DCs), the association of RANKL pathway with Fas-mediated apoptosis is obscure. Here, we found that bone marrow–derived DCs (BMDCs) from the Fas-deficient strain *MRL/lpr* mice, could survive much longer than normal DCs. The expressions of Bcl-x and Bcl-2 and the nuclear transport of NF-κB of RANKL-stimulated BMDCs from *MRL/lpr* mice were significantly upregulated. By contrast, Fas expression of BMDCs from normal C57BL/6 and *MRL*$^{+/+}$ mice was increased by RANKL stimulation, and an enhanced DC apoptosis was found when stimulated with both RANKL and anti-Fas mAb, which was associated with activation of caspase-3 and caspase-9. Furthermore, the expression of FLIP$_L$, an inhibitory molecule against Fas-mediated apoptosis, in normal DCs was significantly decreased by RANKL and anti-Fas mAb. Indeed, the adoptive transfer of RANKL-stimulated DCs resulted in rapid acceleration of autoimmunity in *MRL/lpr* recipients. These findings indicate that the crosstalk between RANKL and Fas signaling in DCs might control immune tolerance. (Blood. 2007;110:242-250)

Introduction

Dendritic cells (DCs) are professional antigen-presenting cells that reside in peripheral tissues in an immature state for optimal antigen uptake and respond to inflammatory signals.[1,2] After capture of pathogen-derived antigens and activation by pathogens, DCs migrate from tissues to the lymphoid organs where DCs become mature and initiate antigen-specific T cells.[1,2] While many subpopulations of DCs have been reported to be heterogeneous in their phenotype and localized in lymphoid tissues, there is general agreement that DCs originate from a hematopoietic progenitor, and that there are 3 DC subtypes, including myeloid DCs ($CD11c^+CD11b^+CD8\alpha^-$), lymphoid DCs ($CD11c^+CD11b^-CD8\alpha^+$), and plasmacytoid DCs ($CD11c^+B220^+Gr\text{-}1^+$), all of which have been recently identified.[3-6]

The lifespan of activated antigen-bearing DCs has been estimated to be as short as 3 days.[7,8] Limiting the lifespan of DCs by means of apoptosis may serve to regulate the availability of antigen for T cells and to control immune responses. An important and well-characterized mechanism for apoptosis in immune cells is mediated by Fas, the death receptor.[9] Although Fas has been implicated in the apoptosis of DCs,[10,11] DCs are known to be resistant to Fas-induced cell death.[12] In addition, it has been reported that the resistance to Fas-induced apoptosis in DCs correlates with the consititutive expression of the Fas-associated death domain–like IL-1β–converting enzyme (FLICE)–inhibitory protein (FLIP) ligand.[13] However, the molecular mechanism for maintenance of DCs through Fas-mediated signals is still unclear.

Receptor activator of nuclear factor (NF)–κB ligand (RANKL),[14,15] a type II membrane protein of the tumor necrosis factor (TNF) family, is expressed on osteoblasts, stromal cells, and activated T cells,[15] and binds to the signaling receptor RANK and the decoy receptor osteoprotegerin (OPG).[15,16] Mice lacking RANKL or RANK display dramatically reduced osteoclastogenesis, show defects in early differentiation of T and B cells, systemic lymph nodes, and fail to develop mammary glands.[17,18] Moreover, recent data have showed that the interaction of Fas ligand and Fas expressed on osteoclast precursors increases RANKL-induced osteoclastogenesis.[19] On the other hand, RANKL-RANK interaction has been shown to prolong the survival of mature DCs, whereas the association of the RANKL pathway with Fas-mediated signals in the activation or function of DCs has been obscure.[15,20]

In this study, to define the molecular mechanism for the autoimmunity by immune dysregulation of DCs through Fas and the RANKL pathway, the *MRL/lpr* mouse strain, an autoimmune-prone strain that has a mutated Fas gene, was used to analyze the immune functions of the DCs and autoimmunity such as rheumatoid lesions.

Materials and methods

Mice

MRL/Mp-lpr/lpr (*MRL/lpr*; aged 4-12 weeks; n = 105), *MRL*$^{+/+}$ mice (aged 4-12 weeks; n = 55), and C57BL/6 (B6; n = 50) mice were purchased from Charles River Japan Inc. (Atsugi, Japan). All mice were maintained in specific pathogen–free conditions in our animal facility, and the experiments were approved by an animal ethics board of Tokushima University (Tokushima, Japan).

Submitted November 28, 2006; accepted March 8, 2007. Prepublished online as *Blood* First Edition paper, March 19, 2007; DOI 10.1182/blood-2006-11-059980.

The online version of this article contains a data supplement.

The publication costs of this article were defrayed in part by page charge payment. Therefore, and solely to indicate this fact, this article is hereby marked "advertisement" in accordance with 18 USC section 1734.

Generation of murine BMDCs

A crude population of DCs was generated in vitro from mouse bone marrow as described with some modifications.[21,22] Briefly, bone marrow was flushed from the long bones of the limbs. Cells were plated at a density of 1×10^6 and were cultured for 7 days in 5% CO_2 at 37°C in RPMI 1640 medium containing 10% heat-inactivated fetal bovine serum (FBS), 100 U/mL penicillin, 10 ng/mL recombinant mouse granulocyte-monocyte colony-stimulating factor (GM-CSF; PeproTech, Le Perray-en-Yvelines, France), and 5 ng/mL mouse IL-4 (PeproTech). DCs ($CD11c^+$ cells, < 70%) including mainly immature DCs (50% $CD11c^+CD86^-$ cells, < 50%) were routinely used for the experiments.

Flow cytometric analysis

Bone marrow–derived DCs (BMDCs) were stained with fluorescein isothiocyanate (FITC)–conjugated anti-CD11c mAb, along with rat anti–major histocompatibility complex class II (MHC class II; $I\text{-}A^k$) as primary Ab and phycoerythin (PE)–conjugated anti-rat IgG as secondary Ab. BMDCs were also stained with PE–anti-CD86, PE–anti-CD80, or anti–Bcl-2, anti–Bcl-xL, and PE–anti-rat IgG. For each staining, isotype-matched mAb was used as a control. All mAbs were obtained from BD Biosciences (San Diego, CA). The cells were analyzed with an EPICS flow cytometer (Beckman Coulter Inc, Miami, FL), and data were analyzed with FlowJo FACS analysis software (Tree Star Inc, Ashland, OR).

Detection of apoptotic cells

Cells were treated with or without 100 ng/mL Fas-activating antibody (Jo-2; BD Biosciences) for 24 to 72 hours and were detected with an EPICS flow cytometer using an Annexin V–FITC apoptosis detection kit (Genzyme, Cambridge, MA). Briefly, after cultured cells were washed in phosphate-buffered saline (PBS), the cells were incubated with FITC-conjugated Annexin-V and propidium iodide (PI) for 10 minutes at room temperature in the dark. Binding buffer was added, and apoptotic cells were detected by flow cytometric analysis with an EPICS flow cytometer.

Measurement of cytokine production

Cytokine production was tested by a 2-step sandwich enzyme-linked immunosorbent assay (ELISA) using a mouse IL-12p40, IL-10, and interferon (IFN)-γ, IL-2, and IL-4 kit (Genzyme, Cambridge, MA). In brief, the culture supernatants from DCs or T cells were added to microtiter plates precoated with anti-IL-12p40, IL-10, IFN-γ, IL-2, and IL-4 capture Ab and incubated overnight at 4°C. After adding biotinylated detecting Ab and incubating at room temperature for 45 minutes, streptavidin-peroxidase was added and incubated again at room temperature for an additional 30 minutes. Finally, an 2,2′-azino-di-3-ethylbenzthiazoline sulfonate substrate containing H_2O_2 was added, and the colorimetric reaction was read at an absorbance of 450 nm using an automatic microplate reader (Bio-Rad Laboratories Inc, Hercules, CA). The concentration was calculated according to the standard curves produced by various concentrations of recombinant cytokines.

MTT assay

The effect of RANKL on proliferation of BMDCs was determined by the MTT dye uptake method. Briefly, the cells (2000/well) were incubated in triplicate in a 96-well plate in the presence or absence of RANKL in a final volume of 0.1 mL for the indicated time periods at 37°C. Then, 0.025 mL MTT solution (5 μg/mL in PBS) was added to each well. After incubation at 37°C for 2 hours, 0.1 mL of the extraction buffer (20% sodium dodecyl sulfide [SDS], 50% dimethylformamide) was added. Incubation was continued overnight at 37°C, and then the optical density (OD) was measured at 450 nm using an automatic microplate reader (Flow, McLean, VA), with the extraction buffer as blank.

Western blot analysis

The cell extracts from the nucleus and cytoplasm of DCs were prepared using the Nuclear/Cytosol Fractionation Kit (Bio Vision, Mountain View, CA). Cells were briefly washed, collected in ice-cold PBS in the presence of phosphatase inhibitors, and centrifuged at 230*g* for 5 minutes. The pellets were resuspended in a hypotonic buffer, treated with detergent, and centrifuged at 14 000*g* for 30 seconds. After collection of the cytoplasmic fraction, the nuclei were lysed and nuclear proteins were solubilized in lysis buffer containing protease inhibitors. A total of 50 μg of each sample per well was used for SDS–polyacrylamide gel electrophoresis. After blocking with 5% nonfat milk, the membrane was incubated with primary antibodies for TRAF6, IKK, p-IκBa, NF-κB p65 (RelA), and p50 (Santa Cruz Biotechnology, Santa Cruz, CA). Antibody-antigen complexes were detected using a horseradish peroxidase–conjugated secondary antibody. Protein binding was visualized with enhanced chemiluminescence Western blotting reagent (Amersham Biosciences, Arlington Heights, IL). Western blotting using anti–Bcl-2, anti–Bcl-xL, anti-Bax, anti-Bid (BD Bioscience), anti–caspase-3, anti–caspase-8, and anti–caspase-9 Abs (Cell Signaling Technology, Beverly, MA), and anti-$FLIP_L$ (Santa Cruz Biotechnology) was performed essentially as described for the lysis buffer. Control for protein loading was provided by anti-mouse histone, or GAPDH mAb (Sigma Chemical Co, St Louis, MO).

siRNA of Fas and RANK

For small interfering RNA (siRNA) of Fas and RANK, a siTrio Full Set (B-Bridge International, Sunnyvale, CA) was used for analyzing the function of DCs. Briefly, each cocktail including the 3 RNA oligonucleotides listed here was transfected into cells with a Silencer siRNA Transfection II kit (Ambion, Austin, TX). Sequences of the oligonucleotide sets are as follows: Fas, GGGAAGGAGUACAUGGACATT (sense), UGUCCAUGUACUCCUUCCCTT (antisense), CGAAAGUACCGGAAAAGAATT (sense), UUCUUUUCCGGUACUUUCGTT (antisense), CCAGAAGGACCUUGGAAAATT (sense), UUUUCCAAGGUCCUUCUGGTT (antisense); and RANK, CCAAGGAGGCCCAGGCUUATT (sense), UAAGCCUGGGCCUCCUUGGTT (antisense), GGGAAAGCGCUGACAGCUATT (sense), UAGCUGUCAGCGCUUUCCCTT (antisense), CUGAAAAGCACCUGACAAATT (sense), UUUGUCAGGUGCUUUUCAGTT. Transfected cells were incubated with or without RANKL, and flow cytometric analysis was performed.

Confocal microscopic analysis

Immature DCs were seeded onto glass-bottom culture dishes (MatTek, Ashland, MA) at a density of 500 cells/well and stimulated for 30, 60, or 120 minutes with RANKL. Subsequently, cells were washed and fixed in cold 3% paraformaldehyde (PFA) in PBS for 10 minutes, then permeabilized with 0.2% Triton-X in PBS for 2 minutes. The slides were then washed thoroughly with PBS and incubated with optimal dilutions of the primary Ab in PBS containing 1% bovine serum albumin (BSA)–2.5% FBS in PBS for 1 hour at room temperature. Cells were stained with optimal dilutions of the primary Abs for 1 hour. After 3 washes with 0.0001% Triton-X in PBS, the cells were stained with Alexa Fluor 488 goat anti-rabbit IgG (H + L; Molecular Probes, Eugene, OR) or Texas red–conjugated goat anti-mouse (Molecular Probes) as the second Abs for 30 minutes and washed with PBS. For each fluorochrome label, negative control Abs were added. Finally, the slides were incubated with 4′, 6-diamidino-2-phenylindole (DAPI) for 5 minutes to label the nuclei and mounted in Vectashield (Vector Labs, Burlingame, CA) for analysis by confocal microscopy (LSM5 PASCAL, Carl Zeiss, Gottingen, Germany). A 63 × 1.4 oil DIC objective lens was used. Quick Operation Version 3.2 (Carl Zeiss) for imaging acquisition and Adobe Photoshop CS2 (Adobe Systems, San Jose, CA) for image processing were used.

Transfer of DCs

BMDCs were stimulated in vitro for 48 hours with 100 ng/mL RANKL and 50 μg/mL bovine type II collagen (CII). RANKL-stimulated BMDCs were transferred into the base of the tail by subcutaneous injections in 200 μL PBS at the age of 4 weeks.

Histopathology

All organs were removed from the mice, fixed with 4% phosphate-buffered formaldehyde (pH 7.2), and prepared for histologic examination. The sections (4 μm in thickness) were stained with hematoxylin and eosin (HE). Histologic grading of inflammatory arthritis was performed according to the methods by Edwards et al[23] as follows: a 1-point score indicates hyperplasia/hypertrophy of synovial cells, fibrosis/fibroplasia, proliferation of cartilage and bone, destruction of cartilage and bone, and mononuclear cell infiltrate. Imaging was analyzed by microscope (BX50, Olympus, Tokyo, Japan) at 20 × 10.70 objective lens. Viewfinder Lite Version 1.0 (Olympus) for image acquisition and Adobe Photoshop CS2 for image processing were used.

Measurement of anti-dsDNA Ab, RF, and CII Ab levels

Anti–double-stranded DNA (dsDNA) Abs, rheumatoid factor (RF), and anti-CII Ab were detected by ELISA as described previously.[11] Briefly, flat-bottom plates (Nalge Nunc International, Roskilde, Denmark) were coated with 1.5 μg/mL of native calf thymus DNA (Life Technologies, Rockville, MD) in buffer containing 0.1 M sodium bicarbonate and 0.05 M citric acid at 4°C overnight. Serum samples were serially diluted (starting at 1:200) and added to the plates for 1 hour of incubation at 37°C. After washing, peroxidase-conjugated goat anti-mouse IgG, or IgM (Southern Biotechnology Associates, Birmingham, AL) was added and incubated for 1 hour at 37°C. Ab binding was visualized using orthophenylenediamine (Sigma Chemical). For the measurement of IgG and IgM RF, human IgG and IgM (Chemicon International, Temecula, CA) were coated onto plates at 10 μg/mL (pH 9.6). The microtiter plate was coated with 100 μL CII antigen solution. After washing 3 times, 100 μL/well of serum samples that had been serially diluted in PBS/Tween 20/1% BSA and control serum samples were added and incubated for 1 hour at 37°C. After washing, peroxidase-conjugated goat anti-mouse IgG (at 1.4 μg/mL, 100 μL/well; Organon Teknika, Durham, NC) was added and incubated for 1 hour at 37°C. A total of 100 μL *o*-phenylenediamine (0.5 mg/mL) dissolved in 0.1 M citrate buffer (pH 5.0) containing 0.012% H_2O_2 was added, and the reaction was stopped using 8 N H_2SO_4 (20 μL/well).

Statistics

The Student *t* test was used for statistical analysis. *P* values greater than .05 were considered significant.

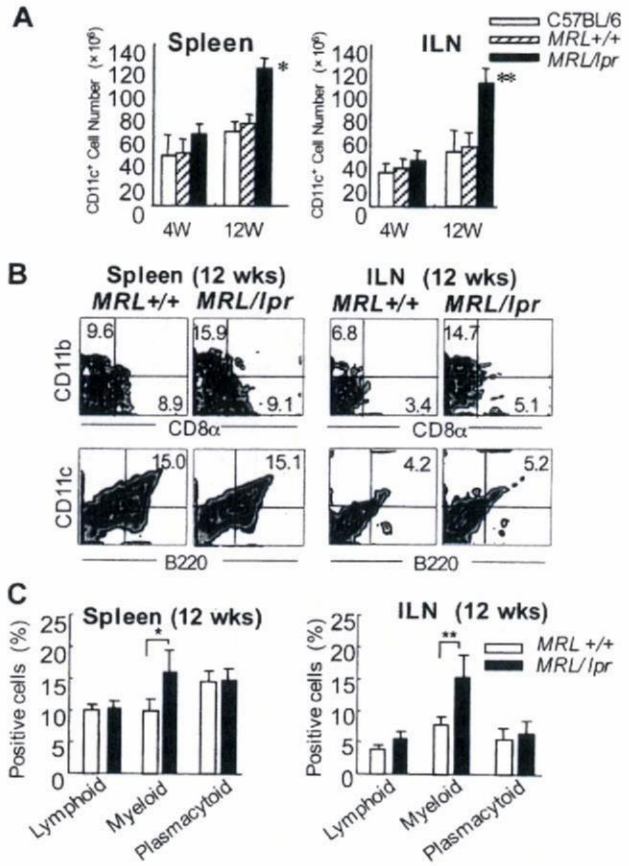

Figure 1. Myeloid dendritic cells in the spleen and inguinal lymph nodes from *MRL/lpr* mice. (A) The CD11c+ DC cell number of the spleen and ILNs is shown as means ± SD of 5 to 7 *MRL/lpr* and control mice at 4 and 12 weeks of age. (B) Mononuclear cells were isolated from the spleen and ILNs at 12 weeks of age, and the proportions were determined using flow cytometry. Shown are representative plots of CD8α+, CD11b+, B220+, and CD11c+ cells. Percentages in each region indicate the frequency of lymphoid (CD11c+CD11b−CD8α+), myeloid (CD11c+CD11b+CD8α−), and plasmacytoid (CD11c+B220+) DCs. Data are representative of 5 to 7 mice in each group. (C) Graph shows the mean frequency of lymphoid, myeloid, and plasmacytoid DCs. *$P > .05$; **$P > .01$ *MRL/lpr* versus $MRL^{+/+}$ mice. Results are representative of 3 independent experiments.

Results

DC numbers and subtypes of *MRL/lpr* mice

To examine the number of DCs from *MRL/lpr* mice, the spleen cells and inguinal lymph node (ILN) cells were analyzed at 4 and 12 weeks of age. We found that the DC number of both spleen and ILNs from *MRL/lpr* mice was significantly higher than that from control mice at 12 weeks of age (Figure 1A). We next analyzed the increased subset of DCs from *MRL/lpr* mice. A significant increase of the myeloid ($CD11b^+CD11c^+CD8\alpha^-$) DC subset of both spleen and ILNs from *MRL/lpr* mice was observed in contrast to the population from control $MRL^{+/+}$ mice, whereas there was no difference in the lymphoid ($CD11c^+CD11b^-CD8\alpha^+$) and plasmacytoid ($B220^+CD11c^+$) DCs between *MRL/lpr* and control mice (Figure 1B-C). Based on these findings, we recognized the possibility that myeloid DCs from *MRL/lpr* mice may have any influence on the immune disorder of the mice.

Activation of RANKL-stimulated DCs from *MRL/lpr mice*

To determine the function of DCs from *MRL/lpr* mice, we generated BMDCs by using the culture of bone marrow cells with recombinant mouse GM-CSF and IL-4. When the cell-surface markers on BMDCs after the culture for 7 days were determined, the myeloid subset DCs from *MRL/lpr* mice had increased significantly compared with that from $MRL^{+/+}$ mice, resembling the phenotype of the spleen and ILN from *MRL/lpr* mice (Figure 2A-B).

Next, activation of the BMDCs from $MRL^{+/+}$ and *MRL/lpr* mice stimulated with RANKL or lipopolysaccaride (LPS) was estimated by analyzing the surface phenotypes, including MHC class II, B7.2 (CD86) and B7.1 (CD80). BMDCs were stimulated with 100 ng/mL mouse recombinant RANKL or 100 ng/mL LPS for 48 hours, and then the surface expressions were detected by flow cytometric analysis as shown in Figure 2C. The expressions of MHC class II, B7.1, and B7.2 on BMDCs from *MRL/lpr* mice in response to RANKL were enhanced compared with those from $MRL^{+/+}$ mice, but no significant difference in the expressions on the BMDCs stimulated with LPS from between $MRL^{+/+}$ and *MRL/lpr* mice (Figure 2C).

This finding indicates that activation of BMDCs from *MRL/lpr* mice via RANKL might be enhanced. In addition, to define the secretion of some cytokines such as IFN-γ, IL-12p40, and IL-10 from RANKL-stimulated BMDCs of *MRL/lpr* mice, BMDCs from

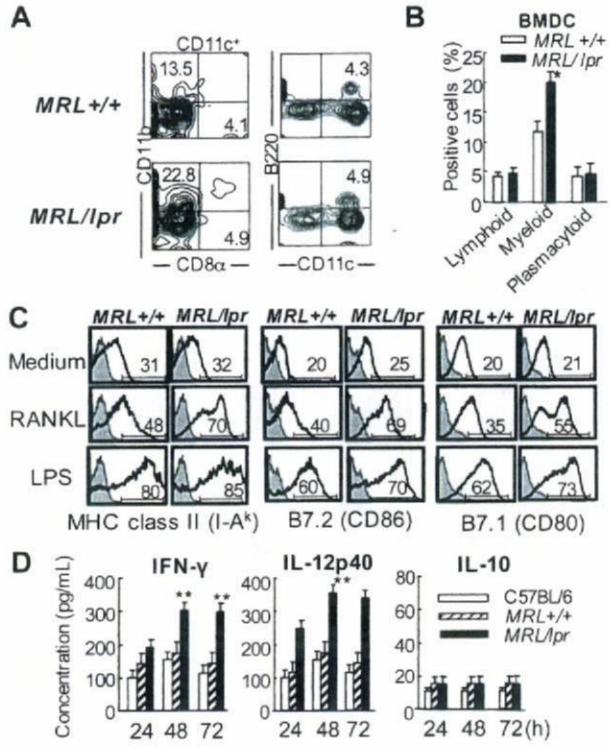

Figure 2. Surface phenotypes and cytokine productions in RANKL-stimulated DCs from *MRL/lpr* mice. (A) BMDCs were generated from *MRL/lpr* and *MRL*$^{+/+}$ mice by using the culture of bone marrow cells with GM-CSF and IL-4 for 7 days; the cell-surface markers of BMDCs were then analyzed. BMDCs from *MRL/lpr* and *MRL*$^{+/+}$ mice were analyzed by flow cytometry. Shown are representative plots of CD8α$^+$, CD11b$^+$, B220$^+$, and CD11c$^+$ cells. Percentages in each region indicate the frequency of lymphoid, myeloid, and plasmacytoid DCs. Results are representative of 3 independent experiments. (B) The graph shows the mean frequency of lymphoid, myeloid, and plasmacytoid DCs. Data are means ± SD of 5 to 7 mice in each group. (C) BMDCs were stimulated with 100 ng/mL mouse recombinant RANKL or 100 ng/mL LPS for 48 hours, and then the surface expressions of MHC class II and costimulatory molecules were detected by flow cytometric analysis. The result is representative of 3 independent experiments. (D) The secretions of IFN-*r*, IL-12p40, and IL-10 in culture supernatants from the BMDCs stimulated by RANKL were detected by ELISA. Data are means ± SD of triplicate samples and are representative of 4 independent experiments. *$P > .05$; **$P > .01$, *MRL/lpr* versus control mice.

normal B6 mice, *MRL*$^{+/+}$, and *MRL/lpr* mice were stimulated with RANKL for 24 to 72 hours, and the cytokine secretion of the culture supernatants was analyzed by ELISA. Significantly increased secretions of IFN-γ and IL-12p40, not IL-10, of BMDCs from *MRL/lpr* mice were observed compared with those from C57BL/6 (B6) and *MRL*$^{+/+}$ mice (Figure 2D). These data suggest that the Fas molecule may influence the activation and function of DCs through RANKL signaling.

Signaling molecules of DCs through RANKL

It is well known that the RANK/RANKL pathway includes a lot of signaling molecules.[24,25] Among them, NF-κB plays a key role for DC maturation and activation.[26] NF-κB activation through RANK/RANKL occurs by nuclear translocation following inducible phosphorylation of inhibitory IκB by IKK complex.[27,28] Therefore, IKKα expression and phosphorylation of IκB (p-IκB) in RANKL-stimulated BMDCs from B6, *MRL*$^{+/+}$, and *MRL/lpr* mice were analyzed by Western blotting. In addition, the expression of TRAF6 downstream from RANK in RANKL-stimulated BMDCs from *MRL/lpr* and control mice was determined.

Increasing expression of TRAF6 after stimulation with RANKL was detected in BMDCs from *MRL*$^{+/+}$ mice. In *MRL/lpr* mice, a much higher expression of TRAF6 in the BMDCs was observed in contrast to that of the control mice. In addition, the expression of IKKα of *MRL/lpr* DCs was up-regulated relative to those of B6 and *MRL*$^{+/+}$ DCs (Figure 3A). Notably, the prominent phosphorylation of IκB of *MRL/lpr* DCs was detected compared with that of control DCs parallel with the increased expressions of TRAF6 and IKKα (Figure 3A). Furthermore, nuclear translocation of NF-κB subunits (p65 and p50) of RANKL-stimulated *MRL/lpr* DCs had increased remarkably compared with that of control DCs (Figure 3B). To define the movements of RANKL-mediated signaling molecules of *MRL/lpr* DCs, the expression of each protein was confirmed by confocal microscopic analysis. Consistent with the results of Western blot analysis using the cytoplasmic and nuclear proteins, the increased nuclear translocation of NF-κB and the up-regulated TRAF6 and p-IκB in the cytoplasm from RANKL-stimulated

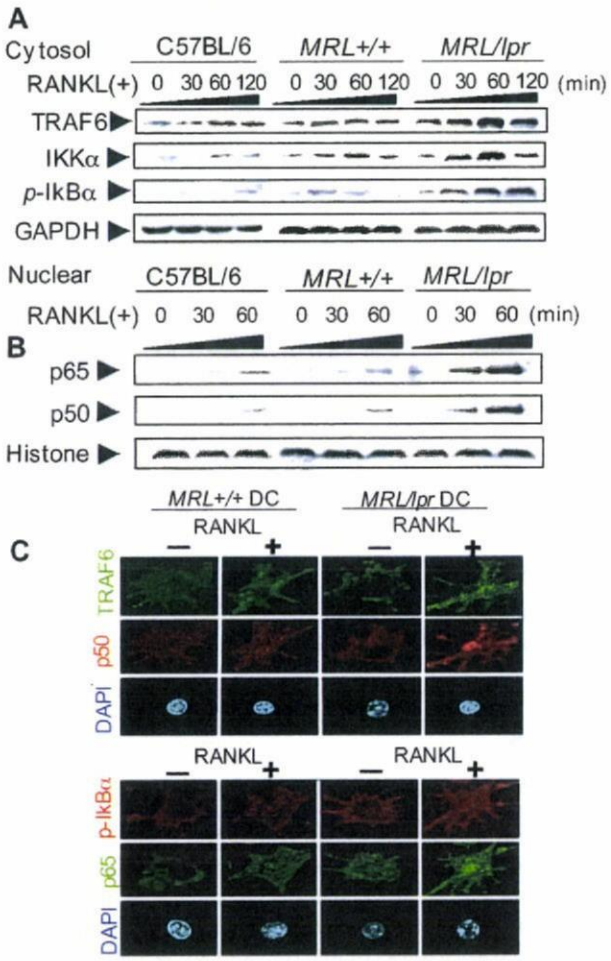

Figure 3. RANKL signaling molecules in *MRL/lpr* DCs. (A) The expressions of TRAF6, IKKα, and phospho-IκB (pIκB) of RANKL-stimulated BMDCs from C57BL/6, *MRL*$^{+/+}$, and *MRL/lpr* mice were detected using the cytoplasmic extracts by Western blot analysis. The BMDCs were stimulated with RANKL (100 ng/mL) from 0 to 120 minutes. GAPDH was used as a housekeeping protein. (B) Nuclear translocation of NF-κB (p65 and p50) of RANKL-stimulated BMDCs from C57BL/6, *MRL*$^{+/+}$, and *MRL/lpr* mice was detected by immunoblot. Histone was used as a housekeeping protein of the nuclear extracts. (C) Increased TRAF6 and p-IκB in the cytoplasm, and accelerated nuclear translocation of p50 and p65 in the nucleus of RANKL-stimulated *MRL/lpr* DCs were detected by confocal microscopic analysis. BMDCs from *MRL/lpr* and *MRL*$^{+/+}$ mice were stimulated for 48 hours with or without RANKL, fixed in 3% PFA on a glass slide, and stained with anti-p65, anti-p50, TRAF6, and p-IκBα followed by Alexa Fluor 488–labeled (green) or Alexa Fluor 568–labeled (red) anti-mouse or anti-rabbit IgG as the second antibodies. The nuclei were stained with DAPI. Original magnification, × 630. All data are representative of 3 to 5 independent experiments.

MRL/lpr DCs were observed in contrast to those from control DCs (Figure 3C). These findings suggest that the Fas molecule might regulate NF-κB activation of DCs through RANKL signaling.

Survival signaling of *MRL/lpr* DCs

To determine the growth of RANKL-stimulated BMDCs from *MRL/lpr* mice, the cell growth was analyzed by MTT assay. At 48 and 72 hours after RANKL stimulation, significantly increased growth of *MRL/lpr* DCs was observed compared with those of B6 and $MRL^{+/+}$ DCs (Figure 4A).

We next analyzed survival signaling molecules, Bcl-xL and Bcl-2, that are antiapoptotic molecules among the Bcl-2 family by flow cytometry. Enhanced expressions of both intracellular Bcl-xL and Bcl-2 in RANKL-stimulated *MRL/lpr* DCs were observed at 24 and 72 hours after the stimulation in contrast to that in $MRL^{+/+}$ DCs (Figure 4B). Moreover, prominent amounts of both Bcl-xL and Bcl-2 in RANKL-stimulated *MRL/lpr* DCs were detected compared with those in $MRL^{+/+}$ DCs using Western blot analysis (Figure 4C). By contrast, the expressions of Bax and Bid, apoptosis signaling molecules, in RANKL-stimulated *MRL/lpr* DCs were lower than those of $MRL^{+/+}$ DCs (Figure 4C). These data suggest

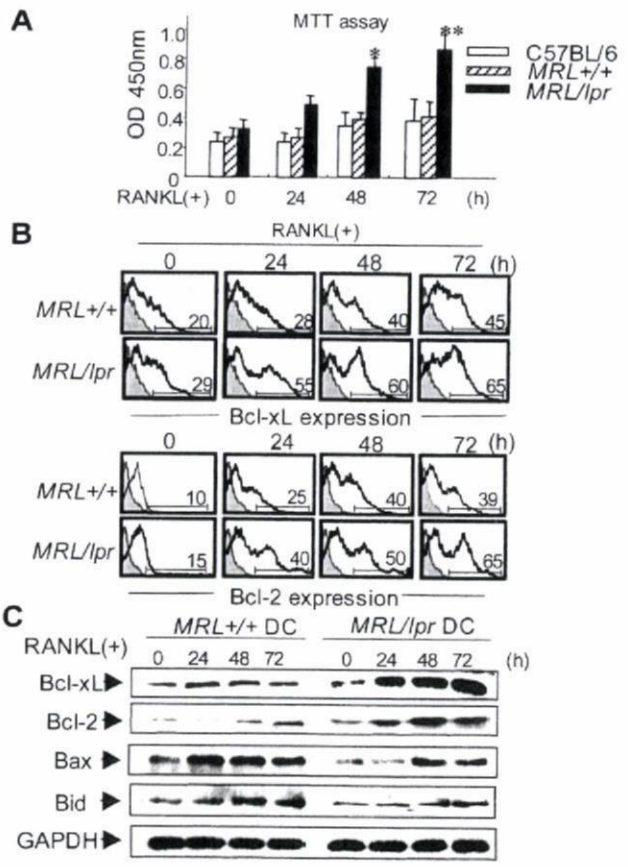

Figure 4. Antiapoptotic signaling through RANKL in *MRL/lpr* DCs. (A) BMDCs were stimulated with 100 ng/mL mouse recombinant RANKL from 0 to 72 hours, and the cell growth was analyzed by MTT assay. Data are means ± SD of triplicate samples and are representative of 4 independent experiments. $^{*}P > .05$; $^{**}P > .01$, *MRL/lpr* versus control mice. (B) BMDCs from *MRL/lpr* and control mice were stimulated with RANKL (100 ng/mL) from 0 to 72 hours, and the intracellular expressions of Bcl-xL and Bcl-2 were analyzed by flow cytometry. Numbers above horizontal lines indicate percent Bcl-xL$^+$ or Bcl-2$^+$ cells. Results are representative of 3 independent experiments. (C) BMDCs from $MRL^{+/+}$ and *MRL/lpr* mice were treated with RANKL (100 ng/mL) from 0 to 72 hours. Bcl-xL, Bcl-2, Bax, and Bid proteins were detected by Western blot analysis. GAPDH was used as a control for loading. Data are representative of 3 independent experiments.

that RANKL signal leads to enhancing the survival of Fas-deficient DCs through up-regulation of antiapoptotic molecules.

RANKL signaling and Fas-mediated apoptosis of DCs

To examine the association of RANKL signaling with Fas-mediated apoptosis in DCs, Fas expression on BMDCs stimulated with RANKL was analyzed. A time-dependent increase in Fas expression on RANKL-stimulated BMDCs from normal B6 and $MRL^{+/+}$ mice, but not *MRL/lpr* mice, was observed (Figure 5A). We found an enhanced apoptosis of DCs when stimulated with both anti-Fas mAb and RANKL, whereas the apoptosis induced by RANKL or anti-Fas mAb was slightly increased (Figure 5B-C). Moreover, to clarify the molecular pathway of enhanced Fas-mediated apoptosis of DCs by RANKL, the movement of caspases downstream from Fas to undergo apoptosis was analyzed using $MRL^{+/+}$ DCs by Western blotting. Although a small amount of cleaved caspase-3 and caspase-9 of RANKL-stimulated $MRL^{+/+}$ DCs was observed, we detected an increased active form of caspase-3 and caspase-9 in the $MRL^{+/+}$ DCs stimulated with both anti-Fas and RANKL (Figure 5D). The activation of these caspases was clearly inhibited by the addition of caspase inhibitor (z-VAD; Figure 5D). Furthermore, the expression of $FLIP_L$, an inhibitory molecule against Fas-mediated apoptosis,[29,30] was significantly decreased by both RANKL and anti-Fas mAb parallel with the movement of the caspases (Figure 5D). It has been reported that $FLIP_L$ is constitutively expressed in DCs to play an inhibitory role for Fas-mediated apoptosis of DCs.[12,13,31] In addition, the expression of pro–caspase-8 was decreased by the stimulation of RANKL or anti-Fas mAb, and the expression was even lower with stimulation by both RANKL and anti-Fas mAb (Figure 5D). For *MRL/lpr* DCs, the expression of $FLIP_L$ was not reduced with RANKL stimulation (Figure 5E). These results strongly suggest that RANKL signaling may contribute to Fas-mediated apoptosis of DCs by controlling the expression of $FLIP_L$.

Effects of Fas siRNA on the function of DCs

To further confirm the enhanced antiapoptotic signal of RANKL-stimulated DCs by Fas deficiency in the *MRL/lpr* mice, we used siRNA of Fas to evaluate the apoptotic signaling and activation of normal BMDCs from control mice.

When BMDCs transfected with the siRNA of Fas were stimulated with RANKL for 48 hours, RANKL-induced Fas expression was decreased to the unstimulated level (Figure 6A). We next examined the inhibitory effect of Fas siRNA on RANKL/Fas-induced apoptosis of BMDCs. As expected, apoptosis of RANKL- and anti-Fas mAb-stimulated BMDCs was clearly inhibited by Fas siRNA, but not GAPDH siRNA or an irrelevant control (Figure 6B). Moreover, to clarify apoptosis signal of RANKL/Fas-mediated apoptosis of DCs, cleavage of caspase-3 was examined using Fas siRNA. A cleaved caspase-3 of BMDCs transfected with control siRNA was detected at 48 and 72 hours after RANKL stimulation, but no active form of caspase-3 of BMDCs transfected with Fas siRNA was observed (Figure 6C).

In addition, to confirm the role of Fas signal for the RANKL-induced activation of DCs, MHC class II expression, as 1 of some activation markers on RANKL-stimulated BMDCs treated with the siRNA, was analyzed by flow cytometry. RANKL-induced expression of MHC class II was still more enhanced by the transfection with Fas siRNA, but not control siRNA (Figure 6D). IL-12 secretion from RANKL-stimulated BMDCs of $MRL^{+/+}$ mice was

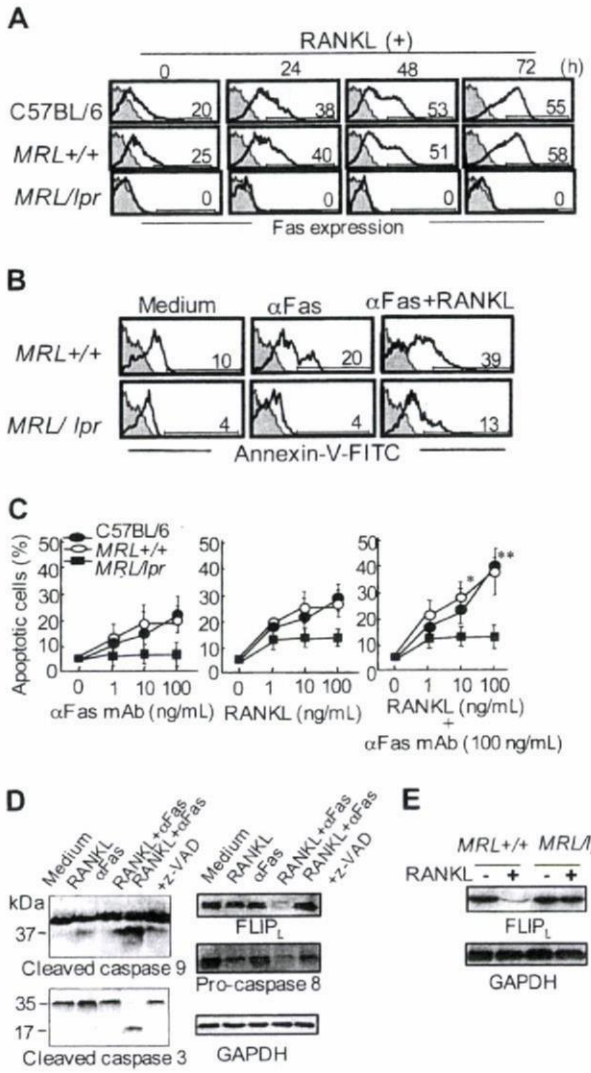

Figure 5. Fas signaling through RANKL in DCs. (A) BMDCs from normal B6, *MRL*$^{+/+}$, and *MRL/lpr* mice were cultured with RANKL from 0 to 72 hours. Fas expression on the DCs was detected by flow cytometry. Numbers above horizontal lines indicate percentage of Fas$^+$ cells. Results are representative of 3 independent experiments. (B) BMDCs from *MRL*$^{+/+}$ and *MRL/lpr* mice were incubated with anti-Fas mAb, or anti-Fas mAb and RANKL, for 48 hours. Apoptotic cells were detected by flow cytometric analysis. Numbers above horizontal lines indicate percentage of Annexin-V$^+$ cells. Results are representative of 3 independent experiments. (C) Apoptotic cells stimulated with anti-Fas mAb (1-100 ng/mL), RANKL (1-100 ng/mL), or RANKL and anti-Fas mAb (100 ng/mL) for 48 hours. B6 (●), *MRL*$^{+/+}$ (○), and *MRL/lpr* (■) mice are shown. Data are means ± SD of 3 independent experiments. $^*P > .05$; $^{**}P > .01$. (D) BMDCs (5×10^4 cells) were cultured treated with RANKL (100 ng/mL) and anti-Fas mAb (100 ng/mL) in the presence or absence of inhibitor z-VAD for 48 hours. The expressions of caspase-9, caspase-3, caspase-8, and $FLIP_L$ of the stimulated BMDCs from control mice were analyzed by Western blot. GAPDH was used as a control for loading. Results are representative of 3 independent experiments. (E) $FLIP_L$ expression of RANKL-stimulated BMDCs from *MRL*$^{+/+}$ and *MRL/lpr* mice was detected by immunoblot. GAPDH was used as a control for loading. Results are representative of 3 independent experiments.

elevated by the treatment with Fas siRNA, indicating that Fas deficiency positively controls RANKL signaling as observed in the DCs from *MRL/lpr* mice (Figure 6E). Moreover, the accelerated nuclear translocation of NF-κB in *MRL/lpr* DCs was observed in RANKL-stimulated BMDCs treated with Fas siRNA (Figure 6F). These findings indicate that RANKL-stimulated DCs from normal mice may be maintained by Fas-mediated apoptosis through caspase and NF-κB cascade.

Inhibitory effect of RANK siRNA on Fas-mediated apoptosis of DCs

To clarify the direct association between RANK/RANKL and Fas signaling of DCs, Fas-mediated apoptosis of RANK-deficient DCs was analyzed using the siRNA of RANK as shown in the protocol (Figure S1A, available on the *Blood* website; see the Supplemental Figures link at the top of the online article). The knockdown of RANK by the siRNA in BMDCs was confirmed by analyzing the protein expression of RANK on flow cytometry and Western blotting as shown in Figure S1B-C. Then, Fas expression and

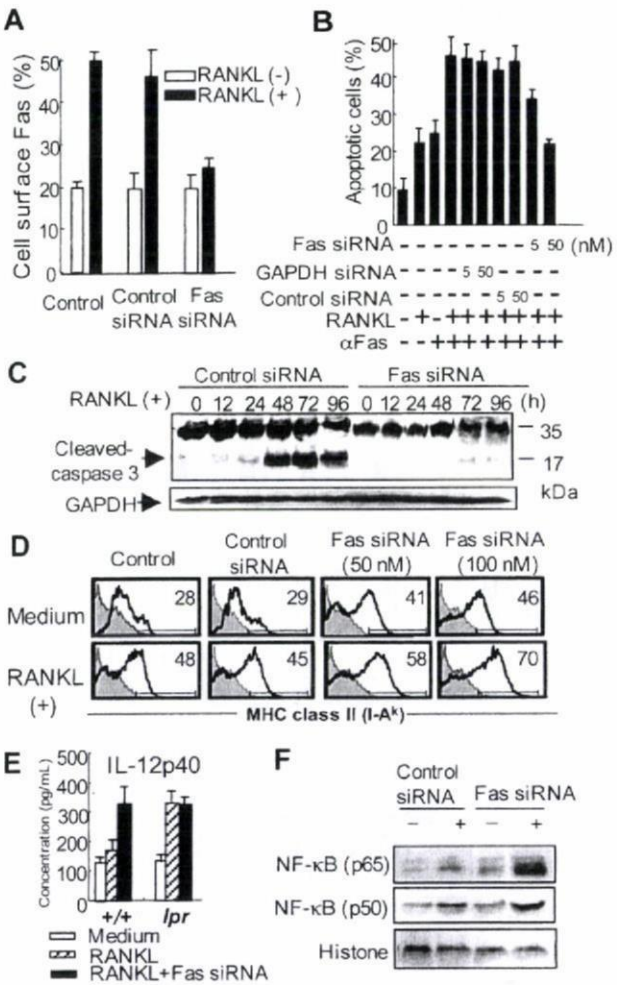

Figure 6. Effects of Fas siRNA on the functions of DCs. (A) Fas expression on Fas siRNA-transfected BMDCs from control mice was analyzed after the stimulation of RANKL. GAPDH siRNA or irrelevant oligonucleotides was used as control. Data are means ± SD of triplicate samples and are representative of 3 independent experiments. (B) Inhibitory effect of Fas siRNA on Fas and RANKL-induced apoptosis of BMDCs from control mice was observed. Apoptotic cells were detected by flow cytometric analysis. Data are means ± SD and representative of 3 independent experiments. (C) Fas siRNA-transfected BMDCs were stimulated with RANKL from 0 to 96 hours. Caspase-3 expression was analyzed by immunoblot. GAPDH was used as a control for loading. Data are representative of 3 independent experiments. (D) MHC class II expression on the Fas siRNA-transfected BMDCs stimulated with RANKL was detected by flow cytometric analysis. Numbers above horizontal lines indicate percentage of MHC class II$^+$ cells. Data are representative of 3 independent experiments. (E) Fas siRNA-transfected BMDCs from *MRL*$^{+/+}$ and *MRL/lpr* mice were stimulated with RANKL, and the secretion of IL-12 from the DCs was detected by ELISA. Data are means ± SD of triplicate samples and are representative of 3 independent experiments. (F) Nuclear translocation of NF-κB subunits (p65 and p50) was detected using the nuclear extracts of Fas siRNA-transfected BMDCs from control mice by Western blot analysis. Histone was used as a control for loading. Data are representative of 3 independent experiments.

apoptosis of RANK-deficient DCs from *MRL*$^{+/+}$ and *MRL/lpr* mice was analyzed as shown in Figure S1D-E. Expectedly, RANKL-induced Fas expression was decreased to the level of unstimulation in RANK-decifient DCs from *MRL*$^{+/+}$ mice (Figure S1D). Furthermore, the Fas- and RANKL-induced apoptosis was reduced to the level of anti-Fas stimulation (Figure S1E).

Influence of activated *MRL/lpr* DCs on arthritis

It is still unclear whether the activated and increased DCs from *MRL/lpr* mice influence autoimmune lesions such as arthritis in the mice. To determine whether the activated DCs from *MRL/lpr* mice may influence autoimmune lesions in vivo, the adoptive transfer of BMDCs stimulated with RANKL and CII into *MRL/lpr* mice at 4 weeks was performed to analyze arthritis lesions of the recipient mice. The histologic score of arthritis in the mice transferred with RANKL- and CII-stimulated *MRL/lpr* DCs was significantly higher at 12 and 16 weeks of age than those of the mice transferred with nonstimulated *MRL/lpr* DCs, RANKL- and CII-stimulated *MRL*$^{+/+}$ DCs, or the untreated mice (Figure 7A). Histologic findings of the recipient mice transferred with RANKL- and CII-stimulated *MRL/lpr* DCs showed severe subsynovial inflammation, synovial hyperplasia, pannus formation, cartilage erosion, and bone destruction (Figure 7B). In contrast, the histology of the mice transferred with RANKL- and CII-stimulated *MRL*$^{+/+}$ DCs was mild, similar to untreated *MRL/lpr* mice (Figure 7B). Anti-CII Ab and RF of sera from the recipient mice transferred with RANKL- and CII-stimulated *MRL/lpr* DCs were significantly increased (Figure 7C). Moreover, increased secretions of IFN-*r* and IL-2, not IL-4 from T cells stimulated with anti-CD3 mAb of the recipient transferred with RANKL- and CII-stimulated *MRL/lpr* DCs, were detected compared with those of the control recipients (Figure 7D). These results indicate that the RANKL-stimulated DCs might play an important role in the acceleration of autoimmune arthritis in *MRL/lpr* mice through T helper 1 (Th1) response.

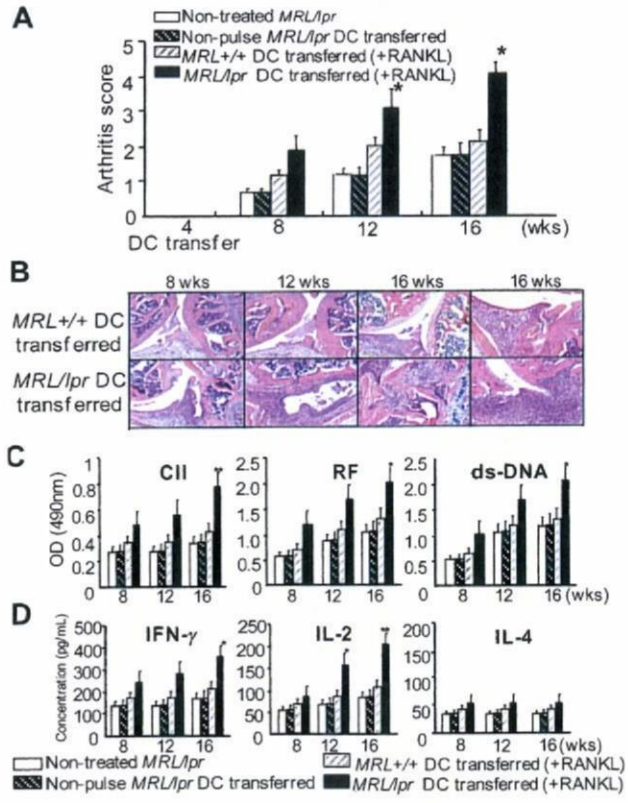

Figure 7. Effects of the RANKL-stimulated *MRL/lpr* DCs transfer on autoimmune arthritis. BMDCs pulsed with CII and stimulated with RANKL were transferred into *MRL/lpr* recipients (4 weeks of age). The recipient *MRL/lpr* mice were analyzed at 8 to 16 weeks of age. (A) Histologic score of autoimmune arthritis in *MRL/lpr* mice transferred with RANKL-stimulated *MRL/lpr* DCs was evaluated compared with control mice until 16 weeks of age. Data are means ± SD of 5 to 7 mice in each group. *$P > .05$; **$P > .01$, *MRL*$^{+/+}$ DCs versus *MRL/lpr* DCs transferred. (B) Histologic analysis of autoimmune lesions from *MRL/lpr* mice transferred with RANKL-stimulated *MRL/lpr* DCs and *MRL*$^{+/+}$ DCs at 8, 12, and 16 weeks of age was performed. The sections of joints from the recipients were stained with HE. Data are representative of 5 to 7 mice in each group. (C) RF, anti-CII antibodies, and anti-dsDNA antibodies of sera from the recipients at 16 weeks of age were detected by ELISA. (D) The secretions of IFN-γ, IL-2, and IL-4 in the supernatants from ILN T cells stimulated with anti-CD3 mAb were detected by ELISA. Data are means ± SD of triplicate samples and are representative of 5 to 7 mice in each group. *$P > .05$; **$P > .01$, *MRL*$^{+/+}$ DCs versus *MRL/lpr* DCs transferred.

Discussion

Studies in the past several years have established an important role of DCs in controlling many immune responses.[1,2] However, the mechanism of maintenance of peripheral DCs has been unclear. The present study indicates that the maintenance of DCs, including cell growth, activation, and apoptosis in the periphery, is regulated by a crosstalk between RANKL and Fas signaling, and that the RANKL/Fas system in DCs may play a key role for the maintenance of peripheral tolerance.

DCs are heterogeneous in terms of phenotype, localization, and function. Several DC subsets have been described based on surface expressions, such as CD11c, B220, CD11b, CD4, and CD8α.[3,4] It has been reported that plasmacytoid DCs induce Th2 cell differentiation in response to certain stimuli, and that myeloid DCs favor a Th1 response.[6] Among myeloid DCs, 4 subsets are known: CD11b$^+$CD8α$^+$, CD11b$^+$CD4$^+$, CD11b$^+$CD4$^-$, and CD11b^{low}CD8α$^-$CD4$^-$.[3,5,6] The function of each subset has been obscure. In this study, increased CD11c$^+$CD11b$^+$CD8α$^+$ myeloid DCs from *MRL/lpr* mice were observed, implying that the maintenance of Th1 DCs in the periphery may occur through Fas signaling, and that Th1 DCs from *MRL/lpr* mice might influence immune disorders such as autoimmune lesions and lymphadenopathy in the mice. It has been described that defective T-cell function of *MRL/lpr* mice plays a key role for pathogenesis of the immune disorder.[10,32,33] Our data demonstrate that dysfunction of DCs from *MRL/lpr* mice accelerates autoimmunity mediated by T and B cells.

It has been reported that the Fas-mediated apoptosis of DCs is resistant due to a constitutive FLIP that can block Fas-induced apoptosis, whereas Fas is expressed on the surface of DCs.[13,31] Upon Fas activation, a set of effector molecules is recruited to the receptor leading to form a signaling complex. Initially, FADD binds to Fas, recruits caspases, and activates a cascade of apoptosis. The present study indicates that Fas-mediated apoptosis of DCs can be induced by the addition of activated RANK/RANKL signaling, suggesting that there may be a crosstalk between the Fas and RANK pathway for DC maintenance in the periphery. In addition, our results indicate that the expression of $FLIP_L$ of DCs is controlled by RANKL and Fas signaling, leading to NF-κB activation. This is consistent with the recent report that cFLIP controls NF-κB activation and maintenance in lymphocytes and DCs.[34] The molecular mechanism may be mediated by activation-induced cell death (AICD), which is well known to act as a system to maintain the peripheral T cells through Fas-mediated apoptosis.[35-37] Activated or autoreactive T cells are considered to delete by

using AICD. Our data suggest that "AICD" of DCs may be mediated by the Fas and RANK pathway.

Bcl-2 family proteins, including Bcl-2 and Bcl-xL, are considered to be critical for DC survival, and to be regulated by NF-κB.[7,38] In this study, Bcl-xL and Bcl-2 expressions of *MRL/lpr* DCs were considerably up-regulated by RANKL stimulation, leading to hyperproliferation of DCs. In addition, NF-κB activation of *MRL/lpr* DCs induced by RANKL was accelerated, suggesting that the Fas signaling pathway might influence NF-κB activation via RANKL signaling in DCs. The NF-κB family has emerged as a key transducer of inflammatory signals to DC maturation and activation, and is well known to be activated by various stimuli such as RANK/RANKL, CD40, and toll-like receptors (TLRs).[14,39,40] Accelerated signaling pathways, including IKKα, IκB, and NF-κB downstream from TRAF6, was observed in *MRL/lpr* DCs stimulated by RANKL. Therefore, RANKL signaling leading to NF-κB activation through TRAF6 in DCs may be regulated by Fas-induced signaling.

DCs are crucial for the pathogenesis of autoimmune disease because of their potent antigen-presenting activity and unique ability to activate naive T cells.[41] DCs have also been described to prime autoreactive T cells and induce the local inflammation of the synovial membrane in arthritis.[42] It was reported that the transfer of collagen-pulsed BMDCs into congenic DBA/1 mice results in inflammatory arthritis.[43] In addition, antigen-pulsed DCs have been shown to induce disease in experimental autoimmune encephalomyelitis, a murine model of multiple sclerosis.[44] Our study showed that transfer of RANKL-stimulated *MRL/lpr* DCs pulsed with collagen into *MRL/lpr* mice clearly accelerates arthritis in the recipients, suggesting that the activated DCs stimulated by RANKL may accelerate autoreactivity of T and B cells to enhance the productions of pathogenic cytokines and autoantibidies in *MRL/lpr* mice. As for autoimmune arthritis of *MRL/lpr* mice, the increased DCs, especially myeloid DCs in the periphery, may play the key role for the pathogenesis. It was previously reported that an imbalance favoring development of DCs from myeloid-committed progenitors predisposes to autoimmune lesion in nonobese diabetic (NOD) mice.[45] Therefore, analyzing the differentiation and function of myeloid DCs may lead to understanding the pathogenic mechanism of autoimmune disease.

Taken together, the new finding in the present study is that the maintenance of DCs, including cell growth, activation, and apoptosis in the periphery, is regulated by crosstalk between RANKL and Fas signaling, and that the RANKL/Fas signaling in DCs may play a crucial role in the maintenance of immune tolerance.

Acknowledgments

The authors thank Ai Nagaoka, Hiroyo Amo, and Satoko Yoshida for technical assistance.

This work was supported by the Ministry of Education, Science, and Culture of Japan (Grants-in-Aid for Scientific Research nos. 17109016 and 17689049).

Authorship

Contribution: T.I. performed all experiments and wrote the manuscript; N.I. codesigned experiments, coperformed confocal microscopic analysis, and wrote the manuscript; K.M. codesigned experiments and wrote the manuscript; M.K. coperformed ELISA with T.I.; R.A. performed Western blot analysis; Y.H. unified the project and wrote the manuscript.

Conflict-of-interest disclosure: The authors declare no competing financial interests.

Correspondence: Yoshio Hayashi, Department of Oral Molecular Pathology, Institute of Health Biosciences, The University of Tokushima Graduate School, 3–18-15 Kuramotocho, Tokushima 770-8504, Japan; e-mail: hayashi@dent.tokushima-u.ac.jp.

References

1. Banchereau J, Steinman RM. Dendritic cells and the control of immunity. Nature. 1998;392:245-252.
2. Banchereau J, Briere F, Caux C, et al. Immunobiology of dendritic cells. Annu Rev Immunol. 2000; 18:767-811.
3. Shortman K, Liu YJ. Mouse and human dendritic cell subtypes. Nat Rev Immunol. 2002;2:151-161.
4. Salomon B, Cohen JL, Masurier C, Klatzmann D. Three populations of mouse lymph node dendritic cells with different origins and dynamics. J Immunol. 1998;160:708-717.
5. Vremec D, Shortman K. Dendritic cell subtypes in mouse lymphoid organs: cross-correlation of surface markers, changes with incubation, and differences among thymus, spleen, and lymph nodes. J Immunol. 1997;159:565-573.
6. Nakano H, Yanagita M, Gunn MD. CD11c(+)B220(+) Gr-1(+) cells in mouse lymph nodes and spleen display characteristics of plasmacytoid dendritic cells. J Exp Med. 2001;194:1171-1178.
7. Hou WS, Van Parijs L. A Bcl-2-dependent molecular timer regulates the lifespan and immunogenicity of dendritic cells. Nat Immunol. 2004;5: 583-589.
8. Matsue H, Edelbaum D, Hartmann AC, et al. Dendritic cells undergo rapid apoptosis in vitro during antigen-specific interaction with CD4+ T cells. J Immunol. 1999;162:5287-5298.
9. Nagata S, Golstein P. The Fas death factor. Science. 1995;267:1449-1456.
10. Chen M, Wang YH, Wang Y, et al. Dendritic cell apoptosis in the maintenance of immune tolerance. Science. 2006;311:1160-1164.
11. Fields ML, Sokol CL, Eaton-Bassiri A, Seo S, Madaio MP, Erikson J. Fas/Fas ligand deficiency results in altered localization of anti-double-stranded DNA B cells and dendritic cells. J Immunol. 2001;167:2370-2378.
12. Ashany D, Savir A, Bhardwaj N, Elkon KB. Dendritic cells are resistant to apoptosis through the Fas (CD95/APO-1) pathway. J Immunol. 1999; 163:5303-5311.
13. Willems F, Amraoui Z, Vanderheyde N, et al. Expression of c-FLIP(L) and resistance to CD95-mediated apoptosis of monocyte-derived dendritic cells: inhibition by bisindolylmaleimide. Blood. 2000;95:3478-3482.
14. Wong BR, Rho J, Arron J, et al. TRANCE is a novel ligand of the tumor necrosis factor receptor family that activates c-Jun N-terminal kinase in T cells. J Biol Chem. 1997;272:25190-25194.
15. Anderson DM, Maraskovsky E, Billingsley WL, et al. A homologue of the TNF receptor and its ligand enhance T-cell growth and dendritic-cell function. Nature. 1997;390:175-179.
16. Simonet WS, Lacey DL, Dunstan CR, et al. Osteoprotegerin: a novel secreted protein involved in the regulation of bone density. Cell. 1997;89: 309-319.
17. Kong YY, Yoshida H, Sarosi I, et al. OPGL is a key regulator of osteoclastogenesis, lymphocyte development and lymph-node organogenesis. Nature. 1999;397:315-323.
18. Fata JE, Kong YY, Li J, et al. The osteoclast differentiation factor osteoprotegerin-ligand is essential for mammary gland development. Cell. 2000;103:41-50.
19. Wu X, Pan G, McKenna MA, Zayzafoon M, Xiong WC, McDonald JM. RANKL regulates Fas expression and Fas-mediated apoptosis in osteoclasts. J Bone Miner Res. 2005;20:107-116.
20. Wong BR, Josien R, Lee SY, et al. TRANCE (tumor necrosis factor [TNF]-related activation-induced cytokine), a new TNF family member predominantly expressed in T cells, is a dendritic cell-specific survival factor. J Exp Med. 1997;186: 2075-2080.
21. Inaba K, Inaba M, Romani N, et al. Generation of large numbers of dendritic cells from mouse bone marrow cultures supplemented with granulocyte/macrophage colony-stimulating factor. J Exp Med. 1992;176:1693-1702.
22. Lutz MB, Kukutsch N, Ogilvie AL, et al. An advanced culture method for generating large quantities of highly pure dendritic cells from mouse bone marrow. J Immunol Methods. 1999;223:77-92.
23. Edwards CK III, Zhou T, Zhang J, et al. Inhibition of superantigen-induced proinflammatory cytokine production and inflammatory arthritis in MRL-lpr/lpr mice by a transcriptional inhibitor of TNF-alpha. J Immunol. 1996;157:1758-1772.

24. Darnay BG, Haridas V, Ni J, Moore PA, Aggarwal BB. Characterization of the intracellular domain of receptor activator of NF-kappaB (RANK): interaction with tumor necrosis factor receptor-associated factors and activation of NF-kappab and c-Jun N-terminal kinase. J Biol Chem. 1998;273: 20551-20555.

25. Wong BR, Besser D, Kim N, et al. TRANCE, a TNF family member, activates Akt/PKB through a signaling complex involving TRAF6 and c-Src. Mol Cell. 1999;4:1041-1049.

26. Ouaaz F, Arron J, Zheng Y, Choi Y, Beg AA. Dendritic cell development and survival require distinct NF-kappaB subunits. Immunity. 2002;16: 257-270.

27. Darnay BG, Ni J, Moore PA, Aggarwal BB. Activation of NF-kappaB by RANK requires tumor necrosis factor receptor-associated factor (TRAF) 6 and NF-kappaB-inducing kinase: identification of a novel TRAF6 interaction motif. J Biol Chem. 1999;274:7724-7731.

28. Baud V, Liu ZG, Bennett B, Suzuki N, Xia Y, Karin M. Signaling by proinflammatory cytokines: oligomerization of TRAF2 and TRAF6 is sufficient for JNK and IKK activation and target gene induction via an amino-terminal effector domain. Genes Dev. 1999;13:1297-1308.

29. Irmler M, Thome M, Hahne M, et al. Inhibition of death receptor signals by cellular FLIP. Nature. 1997;388:190-195.

30. Scaffidi C, Schmitz I, Krammer PH, Peter ME. The role of c-FLIP in modulation of CD95-induced apoptosis. J Biol Chem. 1997;388:1541-1548.

31. Rescigno M, Piguet V, Valzasina B, et al. Fas engagement induces the maturation of dendritic cells (DCs), the release of interleukin (IL)-1beta, and the production of interferon gamma in the absence of IL-12 during DC-T cell cognate interaction: a new role for Fas ligand in inflammatory responses. J Exp Med. 2000;95:1661-1668.

32. Rieux-Laucat F, Le Deist F, Hivroz C, et al. Mutations in Fas associated with human lymphoproliferative syndrome and autoimmunity. Science. 1995;268:1347-1349.

33. Fisher GH, Rosenberg FJ, Straus SE, et al. Dominant interfering Fas gene mutations impair apoptosis in a human autoimmune lymphoproliferative syndrome. Cell. 1995;81:935-946.

34. Golks A, Brenner D, Krammer PH, Lavrik IN. The c-FLIP-NH2 terminus (p22-FLIP) induces NF-kappaB activation. J Exp Med. 2006;203:1295-1305.

35. Chen Y, Inobe J, Marks R, Gonnella P, Kuchroo VK, Weiner HL. Peripheral deletion of antigen-reactive T cells in oral tolerance. Nature. 1995; 376:177-180.

36. Van Parijs L, Ibraghimov A, Abbas AK. The roles of costimulation and Fas in T cell apoptosis and peripheral tolerance. Immunity. 1996;4:321-328.

37. Ishimaru N, Yanagi K, Ogawa K, Suda T, Saito I, Hayashi Y. Possible role of organ-specific autoantigen for Fas ligand-mediated activation-induced cell death in murine Sjogren's syndrome. J Immunol. 2001;167:6031-6037.

38. Hon H, Rucker EB III, Hennighausen L, Jacob J. bcl-xL is critical for dendritic cell survival in vivo. J Immunol. 2004;173:4425-4432.

39. Park Y, Lee SW, Sung YC. Cutting edge: CpG DNA inhibits dendritic cell apoptosis by up-regulating cellular inhibitor of apoptosis proteins through the phosphatidylinositide-3'-OH kinase pathway. J Immunol. 2002;168:5-8.

40. Rescigno M, Martino M, Sutherland CL, Gold MR, Ricciardi-Castagnoli P. Dendritic cell survival and maturation are regulated by different signaling pathways. J Exp Med. 1998;188: 2175-2180.

41. Legge KL, Gregg RK, Maldonado-Lopez R, et al. On the role of dendritic cells in peripheral T cell tolerance and modulation of autoimmunity. J Exp Med. 2002;195:217-227.

42. Thomas R, Davis LS, Lipsky PE. Rheumatoid synovium is enriched in mature antigen-presenting dendritic cells. J Immunol. 1994;152:2613-2623.

43. Leung BP, Conacher M, Hunter D, McInnes IB, Liew FY, Brewer JM. A novel dendritic cell-induced model of erosive inflammatory arthritis: distinct roles for dendritic cells in T cell activation and induction of local inflammation. J Immunol. 2002;169:7071-7077.

44. Menges M, Rossner S, Voigtlander C, et al. Repetitive injections of dendritic cells matured with tumor necrosis factor alpha induce antigen-specific protection of mice from autoimmunity. J Exp Med. 2002;195:15-21.

45. Steptoe RJ, Ritchie JM, Harrison LC. Increased generation of dendritic cells from myeloid progenitors in autoimmune-prone nonobese diabetic mice. J Immunol. 2002;168:5032-5041.

特集I　T細胞レセプターからのシグナル伝達

T細胞レセプターシグナルとNF-κB*

石丸直澄**
岸本英博***
林　良夫**

Key Words：NF-κB, T cell receptor, IκB, activation, NF-κB2(p100/p52)

はじめに

T細胞の活性化や増殖にはT細胞そのものが産生するサイトカインや増殖因子が必須である．そのサイトカインや増殖因子の転写を制御している転写因子の中でもっとも重要な位置に存在しているのがnuclear factor(NF)-κBである．NF-κBは，IL-2をはじめとしたサイトカインおよびサイトカインレセプター，増殖因子，細胞接着分子，細胞周期に関連する遺伝子，アポトーシス関連遺伝子などT細胞の生死にかかわる重要な遺伝子の転写調節を司っている[1]．一般的にT細胞受容体(T cell receptor；TCR)，CD28を中心とした副刺激分子およびサイトカインレセプターなどを介した刺激からさまざまなシグナル分子を経由してNF-κBの内在性阻害因子であるIκBのリン酸化，ユビキチン化および断片化によってIκBから解離したNF-κB分子のヘテロおよびホモダイマーが細胞質から核内に移行し，標的遺伝子上に存在するκBサイトを介して転写が調節され，さまざまな重要因子が合成されT細胞の機能獲得に用いられている．最近，IκBによるNF-κBの制御機構に加えて新たにNF-κB2による調節機構が明らかにされ，自己免疫疾患の病態発症におけるNF-κBシグナルの謎が解き明かされようとしている．

2つのNF-κB経路

転写因子であるNF-κBは免疫細胞における多くの炎症反応を制御している．NF-κBにはN末にDNA結合に重要な共通のRelホモロジー領域を有するNF-κB1(p105-p50)，NF-κB2(p100-p52)，RelA(p65)，RelB, c-Relの5つのサブユニットがあり(図1)，それらのサブユニットがヘテロダイマーあるいはホモダイマーとなり核内移行し，細胞の活性化や増殖などに重要な遺伝子の転写調節を司ることが知られている[2]．NF-κB経路にはNF-κB1とRelAの複合体によって調節される古典的経路(classical NF-κB pathway)と，NF-κB2とRelBの複合体によって調節される非古典的経路(non-classical NF-κB pathway)が報告されている[3](図2)．

TCR/CD3関連シグナルとNF-κB

T細胞では主にTCRからの刺激がさまざまな伝達分子を介して古典的NF-κBの活性化につながることがよく知られている[4]．まず，TCRからの抗原刺激によりTCR/CD3分子複合体に連動してZAP70, Fyn, Vavやposphoinositide 3-kinase

* The critical NF-κB pathway through T cell receptor.

** Naozumi ISHIMARU, D.D.S., Ph.D. & Yoshio HAYASHI, D.D.S., Ph.D.: 徳島大学大学院ヘルスバイオサイエンス研究部口腔分子病態学分野〔〒770-8504 徳島市蔵本町3-18-15〕; Department of Oral Molecular Pathology, Institute of Health Biosciences, The University of Tokushima Graduate School, Tokushima 770-8504, JAPAN
*** Hidehiro KISHIMOTO, M.D., Ph.D.: 東京理科大学生命科学研究所免疫生物学研究部門